WCDMA for Aeronautical Communications

A thesis presented to the faculty of the College of Engineering, Design and Physical Sciences, Brunel University

Master of Philosophy (M.Phil)

ILIAS PETEINATOS

ilias.peteinatos@brunel.ac.uk

December 2014

Local Supervisor: Evangelos A. Kokkinos

Assistant Professor of Applied Science, Department of Electronic Engineering, TEI of Crete

Acknowledgements

First of all, I would like to express my warmest thanks to my Local Supervisor professor Dr. Evangelos Kokkinos for his support and guidance in my whole effort. He has provided me with invaluable advice and motivation throughout my MPhil at Brunel University and without his assistance this thesis would not have been possible. Furthermore, I would like to thank my Supervisor professor Dr R. Nilavalan(Nila) for his understanding and patient throughout this thesis.

I would also like to thank my parents, my sister and my fiancee for their support.

Contents

Abstract

In this thesis, a study of the capacity of a suggested three - dimensional Air-to-Ground cellular system is being made. The Outside Cell Interference Factor (OCIF) is being calculated through simulations for reverse and forward link using seven loops, from the interfering cells around the desired cell for different values of the maximum height of the cell and its radius. Capacity per cell as well as delay and throughput for packet data transmission was calculated for the first time through closed form equations, with the use of the load factor, the activity factor and sectoring gain using the Automatic Repeat Request (ARQ) algorithm for the correction of errors. Moreover, in this thesis, the algorithm which has been created is being analyzed and used for the simulations. Moreover, for the first time, a case study has been made involving the study of capacity of the Air – to - Ground system for the airports of Greece, in three basic scenarios in which the number of the users, the delay and the throughput per cell is being calculated. In the first scenario, we are restricting to the three major airports of the country, while in the second it expands to six airports covering from the radio-coverage side almost all Greece. In the first two scenarios the same cell radius of 175 km is being used, while in the third the radius is reduced to 100 km and the airports are increased to nineteen. In all three scenarios we assume that all the users use the same service. The voice services are also studied of 12.2 kbps and data with transmission rate 64, 128 and 384 kbps. From scenarios 1 and 2 (cell radius 175 km), it was found that we can service at the same time up to 179 voice subscribers per cell at bit rate 12.2 kbps which reduces to 33 users for video call of 64 kbps and in 18 for video call of 128 kbps. In scenario 3 (cell radius 100km), it was found that we can serve at the same time until 126 voice subscribers per cell at bit rate 12.2 kbps which reduces to 23 users for video call of the 64 kbps and in 13 for video call of 128 kbps. In scenario 3 although the capacity per cell is lower than in scenarios 1 and 2, it provides greater total capacity (for all Greece) in relation to these scenarios.

Key words: Air to Ground, aeronautical communications, cellular, interference, WCDMA, OCIF, interference analysis, capacity, data packet, ARQ, RLOS.

Glossary

ACARS	Aircraft Communications Addressing and Reporting System
AMCP	Aeronautical Mobile Communications Panel
ARINC	Aeronautical Radio Incorporated
ARQ	Automatic Repeat Request
ATG	Air To Ground
ATM	Air Traffic Management
CDMA	Code Division Multiple Access
CPDLC	Controller Pilot Data Link Communications
DL	Dowling
EV-DO	Evolution Data Only system
FANS	Future Air Navigation System
GTA	Ground To Air
kbps	kilobits per second
km	kilometers
OCIF	Outside Cell Interference Factor
QoS	Quality of Service
QPSK	Quadrature Phase –Shift Keying
RLOS	Radio Line Of Sight
SITA	Société Internationale de Télécommunications Aéronautiques
UL	Upling
VDL	VHF Digital Link
WCDMA	Wideband Code Division Multiple Access

Table of Figures

Figure 4.20 Throughput in packets per sec as a function of the number of users in the forward link, R_b=128 kbps

Figure 4.21 Throughput in packets per sec as a function of the number of users in the forward link, R_b=384 kbps

List of Tables

Chapter 1: Introduction

1.1 Introduction

The problem which is being studied in this thesis concerns the communications between aircraft passengers with the rest of the world through their mobile phones or through high speed internet, a service which is yet to be provided.

Moreover, today, the contemporary systems of Air Traffic Management and Air Traffic Control have already reached peak conditions in some major airports due to the increasing numbers of flights that have been taking place in the last years. Therefore, the suggested cellular Air to Ground system can be used for communication between aircrafts and the terrestrial systems of management and control of the safety of flights, which through the present technologies have reached saturation point. More specifically, we will be involved in the study of the capacity of the suggested system.

1.2 General background

Controller–pilot data link communications (CPDLC), also referred to as controller pilot data link (CPDL), is a method by which air traffic controllers can communicate with pilots over a datalink system [20].

Today, there are two main implementations of CPDLC:

- The Future Air Navigation System (FANS-1) was originally developed by Boeing, and Airbus as FANS-A, are now commonly referred to as FANS-1/A, and is primarily used in oceanic routes by wide-bodied long haul aircraft. It was originally deployed in the South Pacific in the late 1990s and was later extended to the North Atlantic. FANS-1/A is an Aircraft Communications Addressing and Reporting System (ACARS) based service and, given its oceanic use, mainly uses satellite communications provided by the Inmarsat Data-2 (Classic Aero) service.
- The ICAO Doc 9705 compliant ATN/CPDLC system, which is operational at Eurocontrol’s Maastricht Upper Airspace Control Centre and has now been

extended by Eurocontrol's Link 2000+ Programme to many other European Flight Information Regions (FIRs).

The VDL Mode 2 networks operated by ARINC (Aeronautical Radio Incorporated**)** and SITA (Société Internationale de Télécommunications Aéronautiques) are used to support the European ATN/CPDLC service. The VHF Data Link or VHF Digital Link (VDL) is a means of sending information between aircraft and ground stations (and in the case of VDL Mode 4, other aircraft). Aeronautical VHF data links use the band 117.975–137 MHz assigned by the International Telecommunication Union to *Aeronautical Mobile Services (Route)*. There are ARINC standards for ACARS on VHF and other data links installed on approximately 14,000 aircraft and a range of ICAO standards defined by the Aeronautical Mobile Communications Panel (AMCP) in the 1990s. Mode 2 is the only VDL mode being implemented operationally to support Controller Pilot Data Link Communications (CPDLC).

1.3 Literature survey

The first project which was carried out on this problem, was held by Matolak in 2000 [2], who suggested a three-dimensional cellular cell system for the Air-to-Ground communication. In his paper, he calculated the interference factor which is due to users outside the cell it serves (outside-cell interference factor) of a CDMA system, which comprises of uniformly distributed terrestrial base stations and users who are in aircrafts. It is known that the capacity of the CDMA systems is generally speaking inversely proportional of the outside-cell interference factor. In his paper Matolak shows that the almost free-space transmission environment which exists in the Air-to-Ground model, the interference factor which is due to the users outside the cell, is greater than in the respective terrestrial transmission models (as it can be easily understood because there are no objects which could intervene in the interference signal) and it depends approximately on the algorithm of the radius and the height of the cell.

In 2005, Zhou and his co-workers [3] expanded Matolak's paper with a view to research on the performance in the forward link for transmission data packets, and the capacity, the throughput and the delay of the system were calculated. Their numerical results confirmed Matolak's results, namely that the performance in

aeronautical systems is worse than in the respective terrestrial systems and depends logarithmically on the radius and the height of the cell.

In 2007 Zhou and his co-workers [5] were involved in the impact of the imperfect power control in CDMA Air-to-Ground communications systems. Assuming that the imperfect power control follows log-normal statistics, they studied the capacity and the possibility of non-function (outage probability) of these systems. The numerical results showed that the CDMA Air-to-Ground communication systems are sensitive even in minor errors of the control power. Given that the checking of power in the WCDMA becomes 1500 times per second both in the UL and the DL, in contrast to the IS-95 system (CDMA which was implemented in America as a second generation cellular communication system) in which the control power is 800 times/second in the UL, while in the DL, it is a lot more slower, therefore the WCDMA is expected to be a less vulnerable system in errors of power control, especially in the DL.

Elnoubi in 2005[6] was involved with the expansion of the popular system of mobile GSM communications, so that its subscribers accept and begin calls while they are on the aircraft, having the same SIM card and the same mobile number with the terrestrial systems. In this paper, he did the necessary alternations in the architecture of the GSM and suggested an area of service in space, of multiple layers, namely he divided the value in three cellular cells of the same axis. He calculated the capacity for the suggested GSM system and he compared it with the capacity for CDMA and FDMA systems. The conclusion he drew was that his suggested which system has greater capacity assuming that there is the same bit rate per user in all the systems.

In order to solve the problem of saturation of the existing technologies for the ATM and ATC the STAR project [7] was implemented, in which the performance of the WCDMA system applied in ATM communications was checked by using a demonstrator. The results of the simulations showed that with the use of the WCDMA system in ATM communications we have an increase of the capacity in relation to the existing ATM system VDL mode 2.

Most recently Smida at all [4] provided analytical bounds for the interference between the cells for ground to airborne cellular communication systems, assuming a three-dimensional hexagonal cell pattern. She also assumes that there is line of sight channel without shading and ideal antenna patterns. She also provides numerical

results which show that the bounds are very tight. An implementation which could be accomplished according to Smida is an Evolution Data Only system (EV-DO) Release 0 and Revision A, in which the channels have bandwidth 1.25 MHz both in the forward and the reverse link.

1.4 Motivation

A solution of the problem of saturation which exists in the contemporary systems of Air Traffic Management and Air Traffic Control, can be, the use of WCDMA technology. The WCDMA (Wideband Code Division Multiple Access) was regarded as a possible solution due to its high spectral efficiency and due to the fact that there has been a decade of experience since the development of the terrestrial WCDMA systems worldwide.

In this thesis, a study of the communication between Air to Ground (ATG) and Ground to Air (GTA) for the supply of telephony and data service, is provided. Especially, a capacity study of the airspace of Greece will be given in next chapters, so that the users could use their mobile phones or the Internet during their flights. So far the use of mobile phones and other electronic devices is prohibitted during flight time for security reasons. However, through the course of time (and the increase in the need for communication for personal and professional reasons) the use of all the electronic devices will be allowed making flight time more pleasant and more constructive for the passengers.

1.5 Scope of the thesis

In this present thesis the aim is to study the capacity of the three –dimensional cellular Air-to-Ground system. In order to do that, calculations must be done through simulations of the outside cell Interference Factor (OCIF), for reverse and forward link, by using seven rings of interfering cells around the desired cell, for various values of the maximum height of the cell and its radius.

In this thesis, the question under study is the planning of the capacity in Air-to-Ground communication systems (ATG and GTA) for the supply of telephony and data service.

1.6 Author's research contributions

For the first time, the capacity per cell for Air-to-Ground systems was calculated by using closed form equations through the use of load factor, activity factor and sectoring gain. Moreover, in this thesis, the algorithm which I created and used in the simulations is analyzed while in other papers only the results of the respective algorithms are presented. Furthermore, the delay and throughput for packet data transmission were calculated for the first time for Air-to-Ground systems, through closed form equations, with the use of the load factor, the activity factor and sectoring gain, using Automatic Repeat Request (ARQ) algorithm for the correction of errors. Last but not least, for the first time there has been a case study which involves the study of the capacity of the Air-to-Ground system for the airports of Greece, for three basic scenarios. In this thesis the number of users, the delay and the throughput per cell is calculated. In the first scenario, we are restricted in the three major airports of Greece, while in the second we moved on to six airports covering from radio-coverage side almost all Greece. In both scenarios the same radius cell of 175 km is used, while in the third scenario the radius is reduced to 100 km and the airports are increased to nineteen. In all three scenarios we assume that all users use the same service. We studied voice service 12.2 kbps and data service bit rate 64, 128 and 384 kbps.

1.7 Thesis organization

In current chapter, is shown the thesis Introduction. In chapter 2 the Problem Formulation is presented and more specifically the model of Matolak [2] is being analysed for a cellular system with cellular cells for the Air-to-Ground communication, the equations are given for the calculation of the Outside Cell Interference Factor for reverse and forward link. Moreover, the distance of a user who is in an interfering cell is calculated until the center of the desired cell because it is needed to calculate the OCIF. Next the capacity per cell for reverse and forward link is calculated and the delay and throughput for packet data transmission for forward

link, with the use of load factor, activity factor and sectoring gain. In chapter 3 the algorithm used to calculate the OCIF is explained for both links and its results are given for different values of height and radius of the cell. Moreover, the numerical values for the capacity per cell are calculated for different values of the height and the radius of the cell. In chapter 4, there is a study of the capacity of the Air-to-Ground system for the airports of Greece, for three basic scenarios and the number of users is calculated as well as the delay and throughput per cell.

Finally, in chapter 5, the conclusions of this thesis are presented, derived from our results and some thoughts for future work is given.

Chapter 2: Problem Formulation

2.1 Introduction

Until the present day, the use of mobile phones during flights is prohibited for safety reasons. This is anticipated to change in the immediate future from the one hand due to the increasing need for communication among human beings and on the other hand due to the increasing use of airplanes. The major limiting factor of the capacity of a cellular system is the existence of interference and therefore, there needs to be a quantification of this interference.

2.2 Hexagonal Cell – Concentric cylinder of the same volume

In ground cellular systems, we use cells of regular hexagons. Their expansion for the modeling of the Air to Ground and Ground to Air systems would be the use of regular hexagonal prisms, as can be seen in Figure 2.1

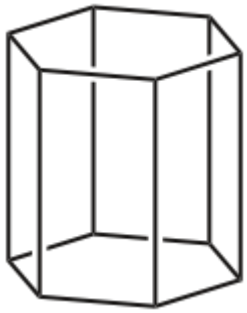

Figure 2.1 Regular hexagonal prism

For reasons of carrying out the mathematical calculations more easily instead of using hexagonal prism cells we can use cylinder cells of the same height and volume, namely the base of the cylinder cells will have the same area with a regular hexagon.

2.3 Matolak's Model

Matolak's three-dimensional model with cellular cells is being used, see Figure 2.2, where there is visual contact without shading and ideal infrastructure of antennas. In most ground cellular systems the path loss alters according to the law

$\frac{1}{d^3}$ or $\frac{1}{d^4}$ (see [1]-[4] references in Matolak). In the air to ground communication environment the transmission path loss follows the $\frac{1}{d^2}$ law [21].

In this case the transmission path loss of the ATG /GTA channel, is inversely proportional with the square of the distance from the transmitter (like free space model).

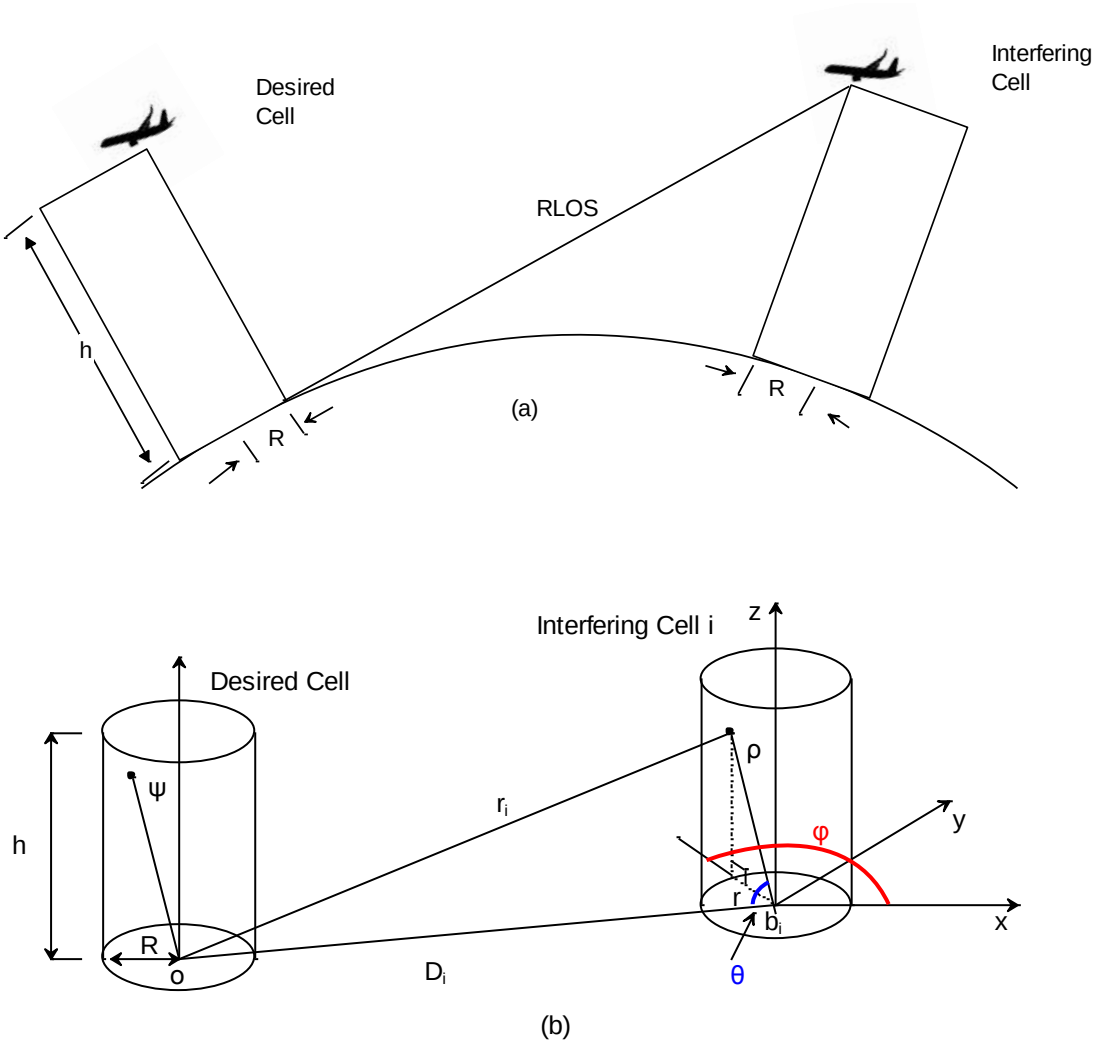

Figure 2.2 The system Air to Ground (a) section (b) 2-D representation, Reverse link.

The base stations, which will be used in this model, will be terrestrial facilities which will be distributed in a similar hexagonal cellular motif, just like those of the

compatible ground cellular systems. From this hexagonal motif we will retain the positions of the base stations. The base stations will be placed in these positions in the Air to Ground model, which will be lain in the centre of the bottom base, of each cylinder.

The mobile stations are airborne and are uniformly distributed in the volume of each cell. Consequently, the hexagonal cell of the conventional terrestrial model is matched with a cylinder in the Air Ground model of the same volume with that of the hexagonal prism. Given that the hexagonal prism would have the same height with the cylinder, in order to have the same volume, they should also have the same base area.

$$E_{circle} = \pi R_{circle}^2 = 2.6\, R_{hex}^2 = E_{hex}$$

$$R_{circle} = 0.9097 R_{hex} \qquad (2.1)$$

In which E_{circle} is the area of the circular base radius R_{cicle}, and E_{hex} is the area of the hexagonal base radius R_{hex}. Because the hexagons are regular the radius R_{hex} of the hexagon is the same with its side.

2.4 Radio Line Of Sight – RLOS

The radio horizon is defined from direct rays of an antenna which are tangential to the surface of the Earth. With the assumption that the Earth is a perfect sphere and if there was no atmosphere, the radio horizon would be a circle.

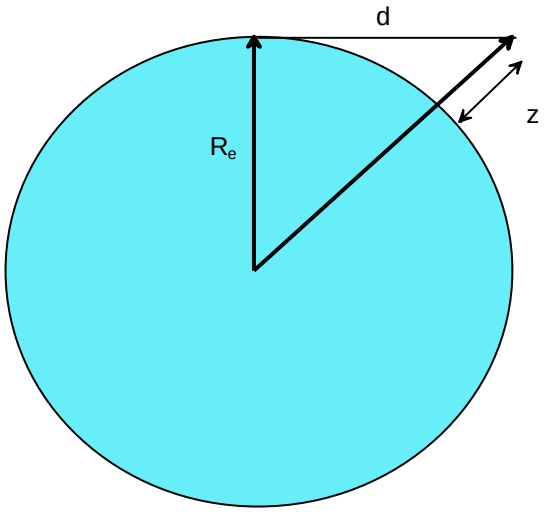

Figure 2.3 Radio line of sight d, for height z from the surface of the earth.

Thus, in Figure 2.3, R_e is the radius of the Earth, R_e= 6.378,135 km, z is the height of the transmitter, d is the line of sight distance.

In reality, the usual effect of the declining pressure of the atmosphere with height is to bend radio waves down towards the surface of the Earth, effectively increasing the Earth's radius, and the distance to the radio horizon, by a factor around 4/3. This factor which is called k-factor can vary from its average value, depending on weather.

Thus, the R_t which is the effective Earth's radius will be

$$R_t = {}^{4}/_{3}\ 6378.135\ \text{Km} \tag{2.2}$$

Suppose that an aircraft is flying at the height z from the surface of the earth. The distance RLOS to the horizon of the earth, for this height z, can be estimated using the Pythagorean theorem in the right-angled triangle OAE as depicted in Figure 2.4, where the length of the line segment AE is the RLOS, (AE) = RLOS. The segment AE is tangent to the surface of the earth and it is perpendicular to its radius.

Therefore, the following can be derived

$$R_t^2 + RLOS^2 = (R_t + z)^2 = R_t^2 + z^2 + 2R_tz \tag{2.3}$$

$$RLOS^2 = z^2 + 2R_tz$$

$$RLOS(z) = \sqrt{z^2 + 2R_tz} \approx \sqrt{2R_tz} \tag{2.4}$$

Because $R_t \gg z \Rightarrow R_tz \gg z^2$

Thus the z^2 can be ignored

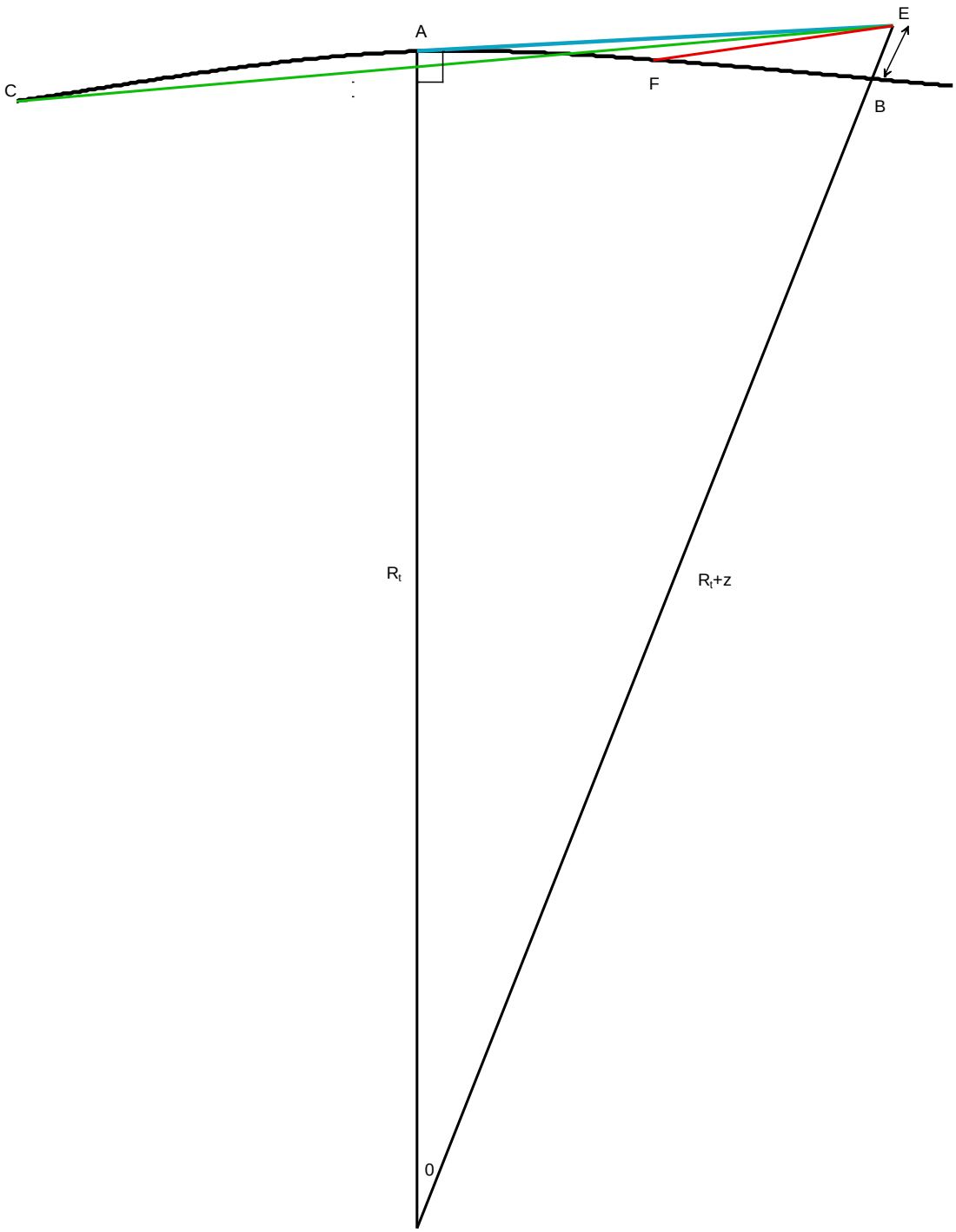

Figure 2.4 Radius of Earth

Let's define the indicator function in which when there is visual contact its value is equal to one, while on the other hand when there is no visual contact, it is zero.

$1, RLOS(z) \geq r_i$

$I(RLOS(z) - r_i) = 0, RLOS(z) < r_i$,

where r_i is the distance from aircraft of interfering cell to the desired cell (see Figure 2.2 b)

We can discern two cases

i) We have visual contact (EF) = r_i as can be observed in Figure 2.4, the (EF) = r_i<RLOS(z)=(AE) =>I (RLOS(z) - r_i) = 1.

ii) We do not have visual contact r_i= (CE) because the visual contact, is being impeded by the curvature of the earth.

(AE)=RLOS(z) <r_i= (CE) =>I (RLOS(z) - r_i) = 0

2.5 Assumptions

Let's assume that the aircrafts are uniformly distributed in the volume of the cell at maximum height H_{max} and each aircraft will be connected to the nearest base station.

Matolak employed omni-directional antennas at the center of each cell. In this thesis the model expanded for the more realistic case of the antenna systems with three sectors (3 sectors) where there is sectoring gain, because the interference which is received from each sector will be the one third of the interference which we would have if we used OMNI antennas. The implementation of sectors will be every 120 degrees. This is done because this way, the periphery of the three sector pattern resembles with the circumference of a circle, see Figure 2.4.1. For simplicity reasons is assumed that the calculation of the OCIF, depends only with the distance from the base station and not by the relative angle. The OCIF, which is the Outside Cell Interference Factor, is an important parameter in defining the capacity of a cellular communication system.

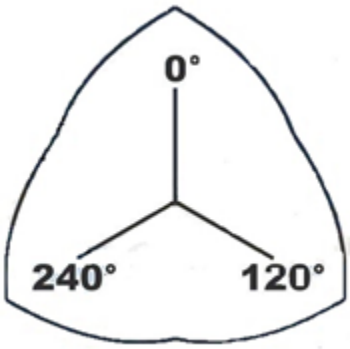

Figure 2.4.1 Three sector antenna pattern

In bisector of two directions of the sectors there will be around 9dB maximum weakening, see i.e at 60 degrees in Figure 2.4.2 from [22], of the signal to the maximum value of the direction. In reality the interference which will be calculated will be higher than the actual one, because it is assumed that the OCIF depends only with the distance from the base station and not by the relative angle.

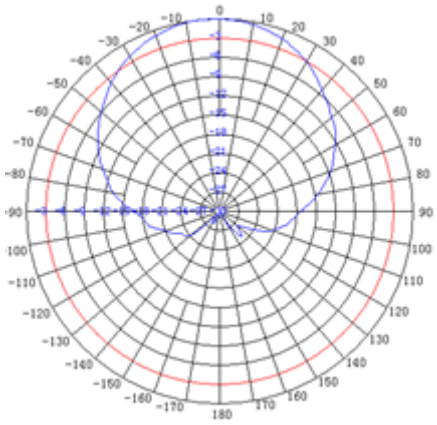

Figure 2.4.2 Horizontal Antenna Pattern of 65 Degree Beamwidth [22]

The basic goal of this research is the calculation of the factors f_R OCIF outside cell in the uplink channel (mobile station to base station) and f_F , OCIF outside cell in the downlink channel (base station to mobile station)

2.6 Calculation of f_R

$$f_R = \frac{Received\ Power\ at\ the\ Base\ Station\ by\ the\ users\ outside\ the\ Cell\ (per\ user)}{Received\ Power\ at\ the\ Base\ Station\ by\ the\ users\ in\ the\ Cell\ (per\ user)}$$

The outside cell interference factor, f_R, is the above ratio of the interference power per user which is received at the base station o from the mobile users outside the cell to the desired power which is received at the base station o from the mobile phones within the cell o, as seen in Figure 2.2.

The factors f_R and f_F are used in evaluating the capacity per cell, namely in calculating the users per cell, in a CDMA system.
According to Viterbi [1], the capacity is:

$$M = \frac{W/R_b}{E_b/N_o} \frac{1}{1+f_R} \tag{2.10}$$

Where,

M: the number of active users

W/R_b: is the bandwidth to data rate transmission ratio

E_b/N_o: is the ratio of the energy per bit of transmitted information to the spectral noise density and interference

f_R: outside cell interference factor

As, in the terrestrial cellular systems, in the downlink channel the transmissions within the cell are synchronous, the MUI is very small. Therefore, the capacity of the downlink channel is greater than the capacity of the uplink channel. Therefore, it is expected that the capacity of the Air – to – Ground system will also be limited by the capacity of the uplink channel.

2.7 Interference caused by the interfering cell i

Every transmission from one user outside the cell, increases the overall Interference. Taking into consideration the transmission path loss in the air - ground environment and therefore the fraction of the distances $(\frac{\rho}{r_i})^2$, as in Figure 2.2 the following equation is obtained [equation (2) in 2],

$$f_{R_i}(h,R) = \iiint_{V_i} \left(\rho/r_i\right)^n I(RLOS(z) - r_i) p(r,\varphi,z) r \, dr \, d\varphi \, dz \tag{2.11}$$

in which cylindrical coordinates are used for, the cylindrical cell.

ρ: the distance of an external mobile station to its own base station.

This is a generic equation as- it is valid for any density function of users $\mathrm{p}(\mathrm{r},\varphi,\mathrm{z})$. In this thesis, as in Matolak's paper [2], the $\mathrm{p}(\mathrm{r},\varphi,\mathrm{z}) = 1/(\mathrm{CellVolume}) = 1/\mathrm{Vi} = 1/(\pi \mathrm{R}^2 \mathrm{h})$ will be used as the spatial density of users, in which h is the height of the cylindrical cell and R is its radius. This ensues the density of users $\mathrm{p}(\mathrm{r},\varphi,\mathrm{z})$ is uniformly distributed, namely it is constant within the volume of the cylindrical cell. Moreover, due to the fact that it is a probability density function (pdf), the (triple) spatial integral in cylindrical coordinates should be equal with 1.

$$\int_0^h \int_0^{2\pi} \int_0^R p(r,\varphi,z) r dr d\varphi dz = 1 \Rightarrow$$

$$p(r,\varphi,z) \int_0^h \int_0^{2\pi} \int_0^R r dr d\varphi dz = 1 \Rightarrow$$

$$p(r,\varphi,z) \int_0^h \int_0^{2\pi} \frac{R^2}{2} d\varphi dz = 1 \Rightarrow$$

$$p(r,\varphi,z) \frac{R^2}{2} \int_0^h \int_0^{2\pi} d\varphi dz = 1 \Rightarrow$$

$$p(r,\varphi,z) \frac{R^2 2\pi h}{2} = 1 \Rightarrow$$

$$p(r,\varphi,z) = \frac{1}{\pi R^2 h} \qquad (2.11a)$$

For the calculation of RLOS the height z in which the airplane flies will be used and not the height h of the cylindrical cell that Matolak uses, because if there is LOS the indicator function I will be one, while if there is no LOS it will be zero and this should solely depend on the height z in which the aircraft flies and not on the height h of the cell.

A similar equation to equation 2.11 is being used in Smida's paper [4] (in which the only difference is, that in this paper the function $\mathrm{I}(\mathrm{RLOS} - \mathrm{r_i})$ is not used in the integral, but the limits of the triple integral change, respectively)

The f_{Ri} is the contribution of the cell i (as in Figure 2.2) to f_R

$$f_R = \sum_{i=1}^{168} f_{Ri}(h,R) \qquad (2.12)$$

As in Matolak's paper it is assumed that the interference for every desired cell o will be estimated that from the 168 cells that surround it, in 7 rings of the cellular pattern. As in Figure 4 of Smida's paper [4], in the first three rings that surround the central cell, which corresponds to the desired cell o of the Figure 2.2: the first ring has 6 cells, second 12 cells and third 18 cells, forth ring 24 cells, fifth 30 cells, sixth 36 cells, seventh 42 cells. As it can be noticed in every following cell, the number of cells increases by 6 cells which surround the central cell.

r_i: the distance of the external user which causes the interference from the base o, n: the path loss exponent of the transmission line = 2 as it was mentioned above, I(RLOS – r_i): is the indicator function to the RLOS, so that when there is Line Off Sight (LOS) between the interfering external user and the base station o, it should contribute in the total interference, while when there is no LOS, it will not contribute.

RLOS has to be calculated based on the height z at which the aircraft flies each time in the same way as it is estimated in Smida's paper. Furthermore, it also defines

$\mathrm{RLOS_{max}} = \sqrt{2\mathrm{R_t}\mathrm{H_{max}}}$ in which the H_{max} is the maximum height of the cell.

2.8 Calculation of the r_i

The r_i is the distance of a user who is in the cell **i** and causes interference at the base station o as in Figure 2.2, can be derived. In Figure 2.5 the projection of the Figure 2.2 is demonstrated on the surface of the earth which is considered to be flat. So, instead of r_i, its projection appears which is the line segment DA.

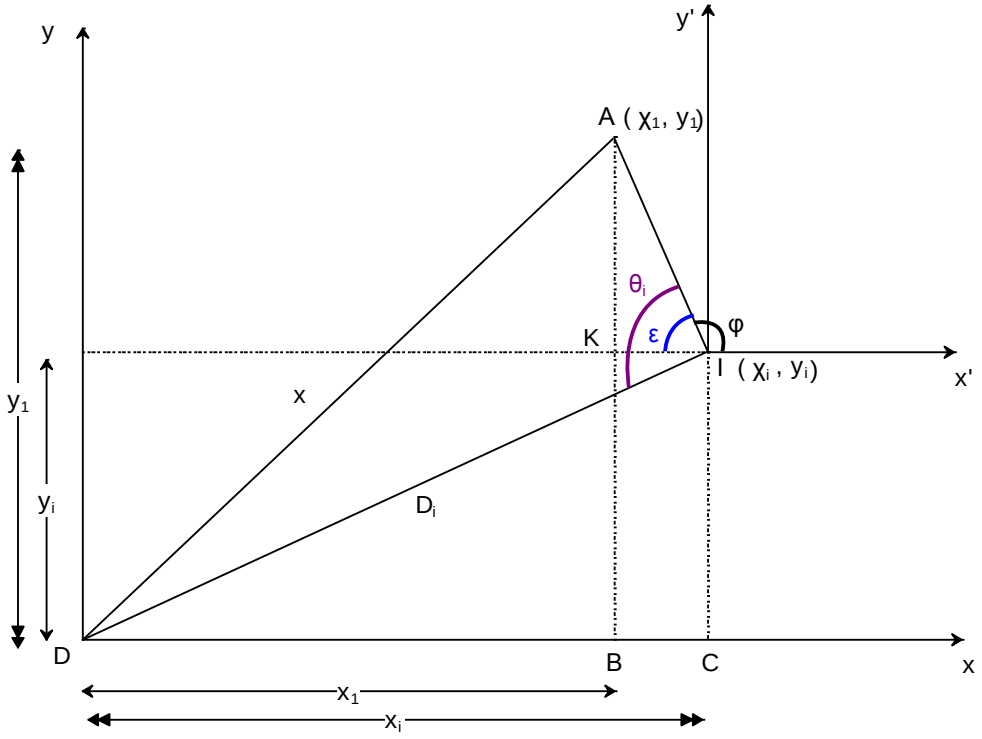

Figure 2.5 The x and y axis of Desire and Interfering Cell on the Earth surface

It is assumed that the coordinate system is centred at D (of the desired cell) and the X-Y axis is at the same level with the coordinate system at center line I (of the interfering cell) and the axis x′y′ parallel to the X-Y axis as it has been depicted in Figure 2.5, namely it is assumed that the earth is flat for the distance between the interference cell and the desired cell.

Point A with coordinates (x_1, y_1) is the projection of the subscriber's terminal who is on an aircraft. The angle φ is the angle which is formed between the axis x′ and r. From the right-angled triangle DIC the Pythagorean Theorem can be derived and it can be derived that:

$$x_i^2 + y_i^2 = D_i^2 \qquad (2.13)$$

It can be assumed that the aircraft is flying at the height z from the surface of the earth which is considered for simplicity being flat in morphology (without hills and mountains). So, since point A is the projection of the subscriber's terminal which is within the aircraft on the surface of the earth, it can be imagined that the right angled triangle which will have as tops the subscriber's terminal which is at the height

z and the two points of our level shape A and D. The hypotenuse of this right-angled triangle is the r_i which has to be estimated and which is given by the relationship:

$$r_i^2 = z^2 + x^2 \tag{2.14}$$

Moreover, from the other right angled triangle DAB,

$$x^2 = x_1^2 + y_1^2 \tag{2.15}$$

If the relationship (2.15) is replaced in the (2.14) there will be

$$r_i^2 = z^2 + x_1^2 + y_1^2 \tag{2.16}$$

The angles φ and ε will be accessory since

$$\varphi + \varepsilon = 180^0$$

It is valid for accessory angles that:

$$\sin\varphi = \sin\varepsilon \quad \text{and}$$
$$\cos\varepsilon = -\cos\varphi$$

In the triangle KIA of Figure 2.5 there will be:

$$(KI) = r\cos\varepsilon = -r\cos\varphi \text{ and}$$
$$(KA) = r\sin\varepsilon = r\sin\varphi$$

From Figure 2.5, it can also be noticed that :

$$x_1 = x_i - (KI) = x_i + r\cos\varphi \tag{2.17}$$
$$y_1 = y_i + (KA) = y_i + r\sin\varphi \tag{2.18}$$

Therefore if the relationships (2.17) and (2.18) are replaced in (2.16) then r_i will become

$$r_i = \sqrt{(x_i + r\cos\varphi)^2 + (y_i + r\sin\varphi)^2 + z^2} \tag{2.19}$$

$$r_i = \sqrt{x_i^2 + r^2\cos^2\varphi + 2x_i r\cos\varphi + y_i^2 + r^2\sin^2\varphi + 2y_i r\sin\varphi + z^2} \tag{2.20a}$$

By using equation (2.13) r_i becomes

$$r_i = \sqrt{D_i^2 + r^2(\cos^2\varphi + \sin^2\varphi) + 2r(x_i\cos\varphi + y_i\sin\varphi) + z^2}$$

and according to the known trigonometric identity

$$\cos^2\varphi + \sin^2\varphi = 1 \qquad (2.20b)$$

and we derive in the final relationship for the r_i

$$r_i = \sqrt{D_i^2 + r^2 + 2r(x_i\cos\varphi + y_i\sin\varphi) + z^2} \qquad (2.21)$$

This result for the r_i is different from the r_i which exists in Matolak's paper [2], even though they are symbolizing the same and the same individual symbols are used in equation (2.21). For this reason, trying to certify the rightness of the formula (2.21), the following proof is submitted below with the equivalent formula which can be found in Smida's paper [4] where it is symbolized with R_i .

2.9 Proof of equivalence

Starting with the formula for the R_i which can be found in Smida's paper [4 see between equation (3) and (4)]

$$R_i = \sqrt{D_i^2 + r^2 + z^2 - 2D_i r\cos\theta_i} \qquad (2.22)$$

By comparing equations (2.21) and (2.22) and given that r_i symbolizes the same with $\underline{R_i}$ so they should therefore be equal, in order to make this happen, then the following relationship should be valid

$$2r(x_i\cos\varphi + y_i\sin\varphi) = -2D_i r\cos\theta_i$$

$$-D_i\cos\vartheta_i = x_i\cos\varphi + y_i\sin\varphi \qquad (2.23)$$

We have concluded to this point, that if equation (2.23) is valid then the equivalence between r_i and R_i will also be valid.

From the non-right angled triangle DIA, using the cosine law [10]

$$x^2 = r^2 + D_i^2 - 2rD_i \cos\theta_i \tag{2.24}$$

From equation (2.15) and the relationships (2.17) and (2.18) we have

$$x^2 = x_1^2 + y_1^2 = (x_i + r\cos\varphi)^2 + (y_i + r\sin\varphi)^2 \tag{2.25}$$

From the relationship (2.24) and (2.25) we get

$$r^2 + D_i^2 - 2rD_i \cos\theta_i = x_i^2 + r^2\cos^2\varphi + 2x_i r\cos\varphi + y_i^2 + r^2\sin^2\varphi + 2y_i r\sin\varphi$$

$$\Rightarrow r^2 + D_i^2 - 2rD_i\cos\theta_i = x_i^2 + y_i^2 + r^2(\cos^2\varphi + \sin^2\varphi) + 2r(x_i\cos\varphi + y_i\sin\varphi) \tag{2.26}$$

By using the relationships (2.13) and (2.20a), the equation (2.26) becomes

$$r^2 + D_i^2 - 2rD_i\cos\ \theta_i = D_i^2 + r^2 + 2r(x_i\cos\varphi + y_i\sin\varphi)$$

With the appropriate simplifications

$$-2rD_i\cos\theta_i = 2r(x_i\cos\varphi + y_i\sin\varphi)$$

And it can be concluded

$$-D_i\cos\theta_i = x_i\cos\varphi + y_i\sin\varphi$$

which is exactly similar to (2.23), which proves it's validity.

In Matolak's paper [2] there is a printing mistake for the r_i equation, for more details see Appendix A.

Also in Zhou's paper [3, equation (2)] in the r_i there is r instead of the symbol r^2 which is the correct one as we can see in equation (2.21).

From Figure 2.2 b and the right angled triangle from Interfering Cell i we have:

$$z^2 + r^2 = \rho^2 \tag{2.27}$$

From the relationship (2.11) for n=2 and by setting specific limits in the triple integral, based on the volume of the cylindrical cell we will have:

$$f_{Ri}(h,R) = \int_0^R \int_0^{2\pi} \int_0^h \frac{\rho^2}{r_i^2} \cdot I(RLOS - r_i)\rho(r,\phi,z)rdrd\varphi dz \quad (2.28)$$

If we replace in the (2.28) the (2.27) and the (2.11a) we will have:

$$f_{Ri}(h,R) = \frac{1}{\pi R^2 h} \int_o^{2\pi} \int_o^R \int_o^h \frac{(z^2+r^2)}{r_i^2} \cdot I(RLOS - r_i)rdrd\phi dz \quad (2.29)$$

Therefore by replacing equation (2.29) in the (2.12) we will calculate the f_R.

2.10 The number of users

According to [8, equation.(8.14)] the relationship which derives for the number of users to the activity factor is found by solving for M (in the book it is symbolized with N)

$$M = \frac{(W/R_b) \cdot n_{UL}}{(E_b/N_o)} \cdot \frac{G_v G_A}{1+f_R} \; in\ reverse\ link \quad (2.30)$$

(the f_R is symbolized with i in the book)

The n_{UL} ratio expresses the telecommunications load cell and takes values less than one. This is for reasons of practical implementation of receivers, for example, should the receiver have finite dynamic range and is stable [1, page 204]. Indicative maximum values that can take the n_{UL} are 0.9 and 0.75,[1].

The (W/R) is the processing gain as above and E_b/N_o is the energy per bit ratio of the transmitted information to the spectral density of the noise and the interference.

G_v: is the gain due to voice or data activity.

Typical value for voice after extensive statistical studies in telephone conversations is $\frac{3}{8}$ [24]. This means that the 37.5% of the time that each speaker speaks in average and there are also periods of time in which neither speaker speaks. In the current

mobile telecommunication networks the discontinuous transmission is already being applied which means that when one of the speakers does not speak, the voice detector can realize it and the mobile phone does not transmit data during this period of time, as a result the total interference is being limited, so therefore the capacity of a CDMA system increases.

The $\frac{3}{8}$ activity factor could be expected to become even smaller in the Air – to –Ground model, due to possible delay in the sound of the other speaker because the transmission distance is significantly greater. Therefore, if we take for example, the radius of a cell of R=200Km the electromagnetic wave will travel this distance twice, until one of the subscribers can listen to the response of the other, therefore the distance that the wave will travel will be 400km and therefore.

$$t_d = \frac{4 \cdot 10^5 m}{3 \cdot 10^8 m/sec} = \frac{4}{3} \cdot 10^{-3} sec = 1.33\, ms$$

So the delay does not seem to be that great, so that it can be noticeable to the subscribers (in the same way as in the satellite communications) and hence it cannot affect the activity factor.

In the value of the voice activity factor 0.375 must be added an overhead 0.17 due to dedicated control signaling channel, thus, v = 0.375 + 0.17 = 0.545 [13].

The gain due to voice or data activity $G_v = \frac{1}{v}$

So $G_v = \frac{1}{v} = \frac{1}{0.545} = 1.8349$ in other words the capacity increases to almost 83.5%.

For data v = $\frac{0.1}{1}$ so in this case G_v will range from 1 to 10.

G_A: is the gain due to antenna sectoring. This gain is derived when a sector antenna is used.

As it has been assumed the users are evenly distributed, therefore each sector antennas takes the interference which is only caused by the users who are in its direction. In this way, the interference is reduced and the capacity per one coefficient increases as much as the G_A. The ideal value of the G_A for 3 sector antennas is 3. In actual implementations this gain can be reduced to for e.g. 1dB as in Viterbi [1, page7] and hence it will become 2.4 from 3 (net number) or for more precise calculations one can take a look at equation (2) of [9]. This happens when the directions of the antennas are not 120 degrees. In chapter 4 of this thesis in which the

case study for Greece is being mentioned, the directions of the sector antennas are taken as 120 degrees, therefore G_A is 3. (ideal value)

$\frac{E_b}{N_o}$ *Requirements for reverse link*

In ground WCDMA systems [8, Table 8.2 page 178] the E_b/N_o requirements range based on the service and the bit rate.

Speech: 5dB

data 144 kbps: 1.5dB

data 384 kbps: 1.0 dB

In this thesis, a 7dB E_b/N_o will be used, which B.T.Ahmed etc[11] had used for the Uplink modeling of **Air to Ground WCDMA voice systems.** This difference of the 2dB in relation to the corresponding ground systems is understandable because in the Air to Ground systems there are more adverse conditions of reception because the speed is greater and therefore the sliding Doppler will be much greater.

Therefore, for the data we can increase the requirement for the E_b/N_o for 2 dB and we will get for Air to Ground systems

data 144kbps: 3.5dB

data 384 kbps: 3dB.

2.11 Calculation of OCIF in the downlink channel WCDMA system air to ground

In this section the performance of the downlink channel in terms of delay, throughput and capacity will be considered.

As mentioned in the introduction, the performance of a WCDMA cellular air to ground system is worse compared to the ground cellular systems and it also depends logarithmically on the radius and the height of the cell.

2.12 Calculation of the f_F (Ground to Air)

In Matolak's [2] analysis for the Forward Channel, it is assumed that all the users transmit and receive at the same data rate R_b, same number of users, m, in each cell and the $\left(\frac{E_b}{N_o}\right)_{eff}$ is the same for all users (an average value).

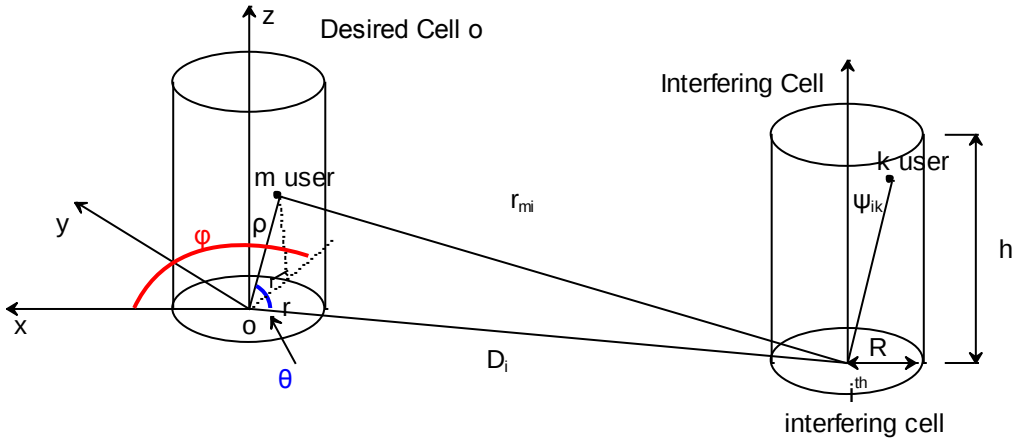

Figure 2.6 Air – Ground model for forward link.

Also for simplicity, Matalok assumes that $\gamma_{om} = \frac{E_{b,om}}{N_o} = \gamma_o$ is the same for all users. Where $E_{b,om}$ is the energy (which the Desired Base Station sends) per bit for the user m.

Therefore

$$\frac{E_{b,im}^{(k)}}{N_o} = \gamma_{om}\left(\frac{\psi_{ik}}{r_{mi}}\right)^2 \tag{2.31}$$

Where, ψ_{ik} is the distance between the i-interfering BS and the k-th user of the i-BS and r_{im} is the distance between the i-interfering BS and the user m in cell o. And $E_{b,im}^{(k)}$ is the interfering power per bit which is received by the m user of the Desired BS.

From Matolak [2, equation 5],

$$\left(\frac{E_b}{N_o}\right)_{eff,m} = \frac{PG\cdot\gamma_o}{\frac{I_{o,m}}{N_o}} \tag{2.32}$$

Where, $PG = {}^{W}/_{R_b}$

$$\frac{I_{o,m}}{N_o} = \gamma_o \sum_{i=1}^{168}\sum_{k=1}^{M}\left(\frac{\psi_{ik}}{r_{mi}}\right)^2 \tag{2.32a}$$

For an average value of $\frac{I_o,m}{N_o}$, we take an expectation, thus

$$\left(\frac{I_o,m}{N_o}\right)_{avg} = \gamma_o M \sum_{i=1}^{168} \mu_i = \gamma_o M \cdot f_F \tag{2.33}$$

Where, 168 cells surround in 7 rings
since

$$f_F = \sum_{i=1}^{168} \mu_i \tag{2.34}$$

$$\mu_i = E\left(\frac{1}{r_{im}^2}\right) \cdot E(\psi_{ik}^2) \tag{2.35}$$

As in Figure 2.6 r_{im} and ψ_{ik} are,

r_{im} : is the distance from the i^{th} interfering base to user m of Desired cell and

ψ_{ik} : is the distance from the i^{th} interfering base to its k^{th} user.

If we substitute equation (2.33) in (2.32),

$$\left(\frac{E_b}{N_o}\right)_{eff,avg} = \frac{PG \cdot \gamma_o}{\gamma_o \cdot M \cdot f_F} = \frac{PG}{M \cdot f_F} \tag{2.36}$$

If we solve for M in equation (2.36),

$$M = \frac{PG}{\left(\frac{E_b}{N_o}\right)_{eff,avg} \cdot f_F} \tag{2.37}$$

Equation (2.37) will give us the capacity of the cell, namely the number of users M, which is the same with equation (8) of Matolak's [2] since equation (2.34) is valid.
In equation (2.37) for reason of simplicity it has been assumed that $G_v = G_A = 1$. Generalizing equation (2.37) both in cases where $G_v \neq 1$ and when $G_A \neq 1$, taking into account equation (1.5) on page 7 of Viterbi [1] which was mentioned in the reverse link and also considering that in the forward link, in place of $(1 + f_R)$, we can use f_F due to the absence of in-cell MUI (As noted by Matolak [2]), it can be concluded that,

$$M = \frac{PG}{\left(\frac{E_b}{N_o}\right)_{eff,avg}} \cdot \frac{G_v G_A}{f_F} \tag{2.38}$$

A corresponding relationship can be derived from equation (8.15) in [8] as observed below, where load is given by n_{DL} in the DL coupling

$$n_{DL} = \sum_{j=1}^{M} v_j \frac{(E_b/N_o)_j}{(W/R_j)} \left[(1 - a_j) + f_{F_j}\right] \quad (2.39)$$

If we match the cases that have been mentioned above, that all users have the same activity factor $v_j = v$, $(E_b/N_o)_j = E_b/N_o$, bit rate $R_j = R_b$, orthogonality factor $a_j = a$ and $f_{F_j} = f_F$ with the user j,

It will become

$$n_{DL} = Mv \frac{(E_b/N_o)}{(W/R_b)} [(1 - a) + f_F] \quad (2.40)$$

and if it is solved for M it will become

$$M = \frac{(W/R_b)n_{DL}}{(E_b/N_o)} \frac{1}{v} \frac{1}{[(1-a)+f_F]} \quad (2.41)$$

Taking into account that the $G_v = \frac{1}{v}$ and if the sectoring gain G_A is also included it will become

$$M = \frac{(W/R_b)n_{DL}}{(E_b/N_o)} \frac{G_v G_A}{[(1-a)+f_F]} \quad (2.42)$$

If it is further assumed that there is complete orthogonality namely a = 1,

$$M = \frac{(W/R_b)n_{DL}}{(E_b/N_o)} \frac{G_v G_A}{f_F} \quad (2.43)$$

By comparing equations (2.38) and (2.43) and assuming the same requirement for the E_b/N_o, $\left(\frac{E_b}{N_o}\right)_{eff,avg} = \frac{E_b}{N_o}$, it can be observed that the (2.38) can give the pole capacity, namely the greatest capacity for $n_{DL} = 1$. Indicatively, the maximum n_{DL} values are: 0.9 and 0.75 for the Uplink.

There can be variations to the f_F, calculations as discussed below:

a) If 3 sectors are configured in a cell, then the numerator of the f_F will become

$$f_F = \frac{\text{interference from other cells}}{\text{interference from subscribers of cell o}}$$

1/3 of the value with an omni also the same thing will happen to the denominator. Hence f_F will be the same. The f_F is symbolized as i in [8, page 184, table 8.7] and it is mentioned that in a macrocell with omni antennas f_F is 55% while with 3 sector antennas it is 65%, in other words there is an increase of 10% because of the increases

in antenna gain compared to the OMNI, hence sectoring affects "interference from other cells" more (i.e., numerator of f_F).

b) Directional antennas used in all 3 sectors but each sector considered as 1 cell. So practically, for 3 sectors, there will be 3 cells.

In this case there is a loss in capacity as can easily be seen in the Erlang B table, but in essence in relation to the OMNI antenna, the numerator of f_F will sub-triple because the interfering aircrafts will be from 120 degrees directions instead of 360 degrees in OMNI case, but the denominator will stay the same (since in each sector is a cell). The increase of f_F due to greater antenna gain compared to the OMNI is less important compared with interference reduction due to sectoring.

If for example there are 100 subscribers per cell, the transmissions of the Base Station (BS) to the 99 subscribers will interfere the 1 subscriber and will create the interference of the denominator of the f_F so the formula for the M in this case will become :

$$M = \frac{(W/R_b)n_{DL}}{\left(\frac{E_b}{N_o}\right)} \cdot \frac{G_v}{\left(\frac{f_F}{n}\right)}$$

$$M = \frac{(W/R_b)n_{DL}}{\left(\frac{E_b}{N_o}\right)} \cdot \frac{G_v n}{f_F} \qquad (2.43a)$$

In which n is the number of the sectors. The above are valid for case b), where for each sector is considered as one cell.

2.13 Calculation of f_F

Equations (2.34) and (2.35) will be used for the calculation of f_F. So, from Figure 2.6 by taking the triple integral on the cylindrical cell we have

$$f_{Fi}(h, R) = \int_o^{2\pi} \int_o^R \int_o^h \frac{E(\psi_{ik}^2)}{r_{im}^2} \cdot I(RLOS - r_{im}) \cdot p(r, \varphi, z) r dr d\varphi dz \qquad (2.44)$$

If equation (2.35) is used then we have

$$\mu_i = f_{Fi}(h, R) = E(\psi_{ik}^2) \int_o^{2\pi} \int_o^R \int_o^h \frac{1}{r_{im}^2} \cdot I(RLOS - r_{im}) \cdot p(r, \varphi, z) r dr d\varphi dz \qquad (2.45)$$

in which $E\left(\frac{1}{r_{im}^2}\right) = \int_o^{2\pi}\int_o^R\int_o^h \frac{1}{r_{im}^2}\cdot I(RLOS - r_{im})\cdot p(r,\varphi,z)rdrd\varphi dz$ (2.46)

2.14 Calculating of $E(\psi_{ik}^2)$

Because, ψ_{ik} in Figure 2.6 is ρ in Figure 2.2b, using (2.27) we have,

$$E(\psi_{ik}^2) = \int_o^{2\pi}\int_o^R\int_o^h (r^2+z^2)\cdot p(r,\varphi,z)rdrd\varphi dz \quad (2.47)$$

From equation (2.11a) we have

$$E(\psi_{ik}^2) = \frac{1}{\pi R^2 h}\int_o^{2\pi}\int_o^R\int_o^h (r^2+z^2)\cdot rdrd\varphi dz \quad (2.48)$$

$$E(\psi_{ik}^2) = \frac{2\pi}{\pi R^2 h}\int_o^R\int_o^h (r^2+z^2)\cdot rdrdz \quad (2.49)$$

$$E(\psi_{ik}^2) = \frac{2\pi}{\pi R^2 h}\int_o^R\int_o^h r^3\,drdz + \frac{2\pi}{\pi R^2 h}\int_o^R\int_o^h z^2\,r\,drdz \quad (2.50)$$

$$E(\psi_{ik}^2) = \frac{2\pi}{\pi R^2 h}\frac{R^4}{4}h + \frac{2\pi}{\pi R^2 h}\frac{R^2}{2}\frac{h^3}{3} \quad (2.51)$$

and so after the simplifications we can concluded that

$$E(\psi_{ik}^2) = \frac{R^2}{2} + \frac{h^2}{3} \quad (2.52)$$

$$\mu_i = f_{Fi}(h,R) = \left(\frac{R^2}{2}+\frac{h^2}{3}\right)\cdot E\left(\frac{1}{r_{im}^2}\right) \quad (2.53)$$

$E\left(\frac{1}{r_{im}^2}\right)$, μ_i and f_F are numerically calculated for all the surrounding cells with the use of Matlab with the use of formulas (2.46), (2.53) and (2.34) respectively.

$$\mu_i = \left(\frac{R^2}{2}+\frac{h^2}{3}\right)\cdot\int_o^{2\pi}\int_o^R\int_o^h \frac{1}{r_{im}^2}\cdot I(RLOS - r_{im})\cdot p(r,\varphi,z)rdrd\varphi dz \quad (2.53a)$$

Because Figures 2.6 and 2.2b are symmetrical r_{im} is calculated with the use of formula (2.21) which gives r_i.

In this thesis, formula (2.38) will be used taking $\left(\frac{E_b}{N_o}\right)_{eff,avg}$ as an independent variable, and M will be calculated for several values of R and h. Specifically for voice services $\left(\frac{E_b}{N_o}\right)_{eff,avg} = 7dB$. For data services $\left(\frac{E_b}{N_o}\right)_{eff,avg}$ is assumed to be 2 dB more than the value of tables found in [8], for the different data rates, in the same way as what happened in the reverse link. In an equivalent way someone could find $\left(\frac{E_b}{N_o}\right)_{eff,avg}$ using M as a free variable. As Matolak mentions in [2, equation 9], in this case, this inequality, in the equal will take its minimum value and so it would give the lower bound, due to the use of 'Jensen inequality' in the curve function $\left(\frac{E_b}{N_o}\right)_{eff,avg} = \frac{PG \cdot \gamma_0}{I_{0,m}/N_0}$ [2, equation 5]. The last one is a convex function, because it is in the form a/x, with $a = PG \cdot \gamma_0 > 0$ and $x > 0$.

Below we will calculate M for both Forward and Reverse Links, and we will compute the minimum M, so we will find which coupling finally sets the limitation (bottle neck). The $(Eb/No)_{eff,avg}$ values will be taken both for the Forward and the Reverse Link from Tables 11.21 and 11.19 respectively in [8] that are valid for terrestrial systems, in case we have multipath fading channel (Case 3 in [8]), in which the user is moving in 120 km/h, are augmented by 2dB, as in [11], due to the adverse conditions of transmission (greater speed, therefore greater Doppler Shift).

As Matolak [2] mentions in his introduction for the forward link, the capacity is calculated as the minimum of (M_s .M) in which M_s is the number of the available synchronous orthogonal spreading codes and M is the number of users which derives from formula (2.38) and where the minimum value of the M_s and M can be taken.

2.15 Packet Data Transmission

In a system where multimedia services are required such as Internet surfing, email, etc., there are asymmetric services (between upload-download) at real or non-real time, the greatest factors with which the output is evaluated are the following:

The Capacity of the system M: the maximum number of active users per cell, in which the required levels QoS (the quality of service) are maintained for a specific error rate bits (BER)

Throughput S: the total number of correctly received data (bits) per seconds in the receiver.

Average delay D: the average time of the data packet transmission, is given by the relationship

$$D = \frac{D\min}{1-P\mathrm{PER}} \tag{2.54}$$

in which D_{min} is the minimum time of transmission packet of length L, it includes the time of packetizing, and the time t_d which is the transmission and processing time.

$$D_{min} = \frac{L}{R_b} + t_d \tag{2.55}$$

in which R_d is the data rate and finally P_{PER} is the packet error rate.

If 100 packets are transmitted, which will have been correctly transmitted will be $100(1- P_{PER})$.

It will take time $100\left(\frac{\mathrm{L}}{R_b} + \mathrm{t_d}\right)$, where $\left(\frac{\mathrm{L}}{R_b} + \mathrm{t_d}\right)$ is the time of 1 packet.

So therefore for the Average Value of delay per packet it will be

$$\mathrm{D} = \frac{100\left(\frac{\mathrm{L}}{R_b} + \mathrm{t_d}\right)}{100\ (1-\mathrm{P_{PER}})}$$

$$\mathrm{D} = \frac{\frac{\mathrm{L}}{R_b} + \mathrm{t_d}}{(1-\mathrm{P_{PER}})} \tag{2.55a}$$

2.16 System Capacity M

In order to calculate the capacity of the system, namely the number M of the active users of a cell the formula (2.30) for reverse link will be used

$$M = \frac{\left(W/R_b\right)\cdot n_{UL}}{(E_b/N_o)} \cdot \frac{G_v G_A}{1+f_R} \quad \text{for reverse link,}$$

while the formula (2.43):

$$\mathrm{M} = \frac{(\mathrm{W}/R_b)\mathrm{n_{DL}}}{(\mathrm{E_b}/\mathrm{N_o})} \frac{G_v G_A}{\mathrm{f_F}} \quad \text{for forward link}$$

2.17 Calculation of Average delay D

One of the basic modulation formats employed in WCDMA is QPSK-Quadrature Phase –Shift Keying [12]. We will examine the BER-Bit Error Rate, namely the possibility of error, which is given by the relationship

$$P_e = Q\left(\sqrt{\frac{2E_b}{N_o}}\right) = \frac{1}{2}\operatorname{erfc}\left(\frac{\sqrt{\frac{2E_b}{N_o}}}{\sqrt{2}}\right) = \frac{1}{2}\operatorname{erfc}\left(\sqrt{\frac{E_b}{N_o}}\right) = P_{BER} \quad (2.56)$$

Equation (2.56) is also valid for BPSK (which is used up to release 6, in the UL[8]) as well as QPSK,

where $$Q(x) = \frac{1}{\sqrt{2\pi}}\int_x^{\infty} e^{-t^2/2}\,dt = \frac{1}{2}\operatorname{erfc}\left(\frac{x}{\sqrt{2}}\right),\ x \geq 0 \quad (2.57)$$

It will be assumed that our packet has L bits. In order to calculate the possibility P_{PER} of the error packet, we will first find the possibility not to have any error in the packet. The $(1 - P_{BER})$ is the possibility of the correct transmission (without Error) of one bit, while $(1 - P_{BER})^L$ is the possibility of correct transmission of the L bits, namely of all the bits of the packet, so this possibility will be equal with the possibility of the correct transmission of the packet $(1 - P_{PER})$.
So there will be

$$P_{PER} = 1 - (1 - P_{BER})^L \leftrightarrow (1 - P_{BER})^L = 1 - P_{PER} \quad (2.58)$$

So if we solve (2.58) for P_{PER} and we replace the P_{PER} from the (2.56) there will be

$$P_{PER} = 1 - \left(1 - \frac{1}{2}\operatorname{erfc}\left(\sqrt{\frac{E_b}{N_o}}\right)\right)^L \quad (2.59)$$

2.18 Reverse link

From equation (2.30) if we solve for E_b/N_o there will be

$$(E_b/N_o) = \frac{(W/R_b)\cdot n_{UL}}{M} \cdot \frac{G_v G_A}{1+f_R} \text{ for reverse link} \quad (2.60)$$

In equation (2.59) E_b/N_o will be replaced by (2.60) and there will be

$$P_{PER} = 1 - \left(1 - \frac{1}{2}\operatorname{erfc}\left(\sqrt{\frac{\left(W/R_b\right)\cdot n_{UL}}{M} \cdot \frac{G_v G_A}{1+f_R}}\right)\right)^{L} \qquad \textit{Reverse link} \qquad (2.61)$$

Delay D for a data packet is derived from equation (2.54) and (2.55) and (2.61) as follows:

$$D = \frac{\frac{L}{R_b} + t_d}{\left(1 - \frac{1}{2}\operatorname{erfc}\left(\sqrt{\frac{\left(W/R_b\right)\cdot n_{UL}}{M} \cdot \frac{G_v G_A}{1+f_R}}\right)\right)^{L}} \qquad \textit{Reverse link} \qquad (2.62)$$

Let's assume that for the correction of the errors in the wireless coupling the ARQ(Automatic Repeat Request) algorithm is being used. The packets which are transmitted in our channel are symbolized with K_d and are the sum of the new packets and the packets which are re-transmitted because in these, error in the receiver can be detected.

$$K_d = K\frac{R_b}{L} \qquad (2.63)$$

In which $\frac{R_b}{L}$ expresses the number of packets of length L per sec and per user, and K is the number of active users. Moreover, $(1 - P_{PER})$ expresses the percentage of the packets which were correctly transmitted.

Throughput S, which is calculated in packets per sec, can be written

$$S = K_d(1 - P_{PER}) = K\frac{R_b}{L}(1 - P_{PER})$$

$$S = K\frac{R_b}{L}\left(1 - \frac{1}{2}\operatorname{erfc}\left(\sqrt{\frac{\left(W/R_b\right)\cdot n_{UL}}{M} \cdot \frac{G_v G_A}{1+f_R}}\right)\right)^{L} \qquad \textit{Reverse link} \qquad (2.64)$$

2.19 Forward link

And from formula (2.43) if we solve for E_b/N_o there will be

$$(E_b/N_o) = \frac{(W/R_b)n_{DL}}{M}\ \frac{G_v G_A}{f_F} \qquad \textit{for forward link} \qquad (2.65)$$

In equation (2.59) E_b/N_o is replaced by the (2.65) and there will be

$$P_{PER} = 1 - \left(1 - \frac{1}{2}\text{erfc}\left(\sqrt{\frac{\left(W/R_b\right)\cdot n_{DL}}{M} \cdot \frac{G_v G_A}{f_F}}\right)\right)^{L} \quad \textit{Forward link} \qquad (2.66)$$

Delay D for a data packet is derived by the equations (2.54) and (2.55) and (2.66) as follows:

$$D = \frac{\frac{L}{R_b} + t_d}{\left(1 - \frac{1}{2}\text{erfc}\left(\sqrt{\frac{\left(W/R_b\right)\cdot n_{DL}}{M} \cdot \frac{G_v G_A}{f_F}}\right)\right)^{L}} \quad \textit{Forward link} \qquad (2.67)$$

As it was mentioned in the reverse link for the correction of the error of the wireless coupling ARQ algorithm is being used.

Therefore, if we assume that our packet has length L, the bit rate is R and is the same for all the users and K is the number of active users in which K ≤ M and M is the maximum number of users/cell, the throughput S (in packets per sec per cell) can be written

$$S = K\frac{R_b}{L}\left(1 - \frac{1}{2}erfc\left(\sqrt{\frac{\left(W/R_b\right)\cdot n_{DL}}{M} \cdot \frac{G_v G_A}{f_F}}\right)\right)^{L} \quad \textit{Forward link} \qquad (2.68)$$

2.20 Summary

The Problem Formulation was presented and more specifically the model of Matolak has been analysed for a cellular system with cellular cells for the Air-to-Ground communication, the equations are given for the calculation of the Outside Cell Interference Factor for reverse and forward link. Moreover, the distance of a user who is in an interfering cell was calculated until the center of the desired cell because it is needed to calculate OCIF. Next the capacity per cell for reverse and forward link was calculated together with delay and throughput for packet data transmission for forward link, using load factor, activity factor and sectoring gain.

Chapter 3: Numerical Results

3.1 Introduction

The algorithm which has been created is analyzed and used for the simulations. Furthermore, the delay and throughput for packet data transmission are calculated, with the use of the load factor, the activity factor and sectoring gain using the Automatic Repeat Request (ARQ) algorithm for the correction of errors.

3.2 Illustration of Calculation Algorithm of f_R and f_F

Let's assume that we have a desired cell o (in the center of Figure 3.1). Around the desired cell, we will assume seven rings, as it had been mentioned in Chapter 2, from interfering cells. We are interested to calculate the distance D between the desired cell o and each interfering cell with the use of the shift parameters (i, j) where i, j are integers. Let's take a side, randomly, of the desired cell o. The vertical in this side is the axis movement of i, and the value of i, expresses how many cell positions we move over this axis. The direction of j derives, if from the direction of i, we turn for 60 degrees anticlockwise and the value of j, expresses how many cell positions we move over this axis. So, from the desired cell o, we have moved in the current interfering cell with use of the shift parameters (i, j).
The distance D between the desired cell and the interfering cell is given [14]

$$D = \sqrt{3}\sqrt{(iR + \cos(60^o)\, jR)^2 + (\sin(60^o) jR)^2} \quad (3.1a)$$

$$D = 1.732\sqrt{(iR + 0.5 \cdot jR)^2 + (0.866 \cdot jR)^2} \quad (3.1b)$$

In reference [14], the author concludes in the well-known result for cellular systems

$$D = R\sqrt{3N} \quad (3.2)$$

where

$$N = i^2 + ij + j^2 \quad (3.3)$$

In the calculation of f_R, f_{Ri} is calculated using equation (2.11) for each one of the 168 interfering cells (seven rings) and then, equation (2.12) is employed to calculate f_R. The scanning mode of these 168 cells is done with the use of two 'for loops' which can be seen in the part of the code which appears on Table 3.1. More specifically, if we take each one of these six sides of the desired cell o, and we draw the vertical lines to these sides, the interfering cells are divided in six sectors as can be seen in Figure 3.1

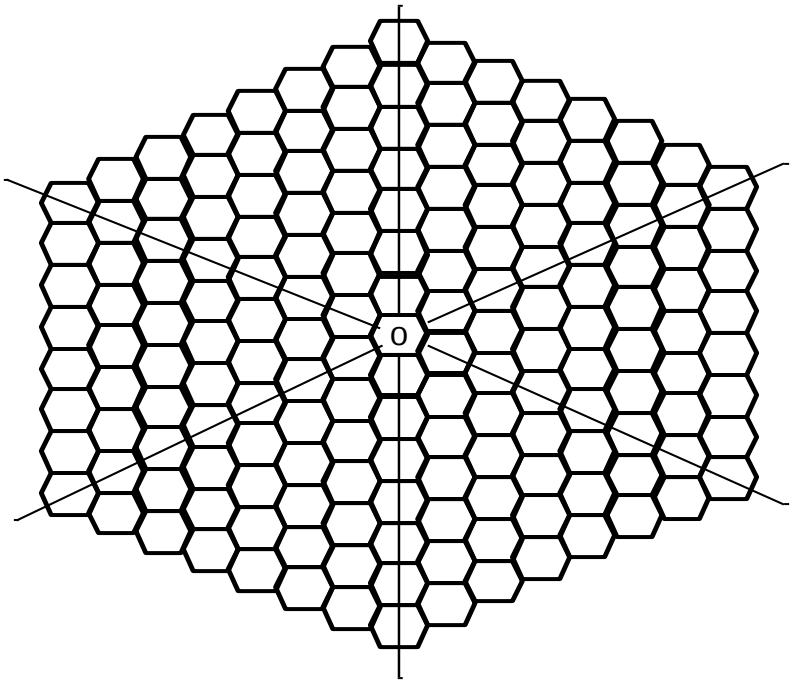

Figure 3.1 The cell pattern with the central cell o which is the Desire cell and around it there are 7 rings of interfering cells

Without loss of generality we can focus on one of these six sectors, if for example we refer to the sector from 300 to 360 degrees (top left sector). The increase of degrees became clockwise, taking as a starting point the north semi axis, namely 0 degrees.
In the first for loop the indicator i begins from the value 7 and in the second for loop the indicator j takes only zero price, see Figure 3.2

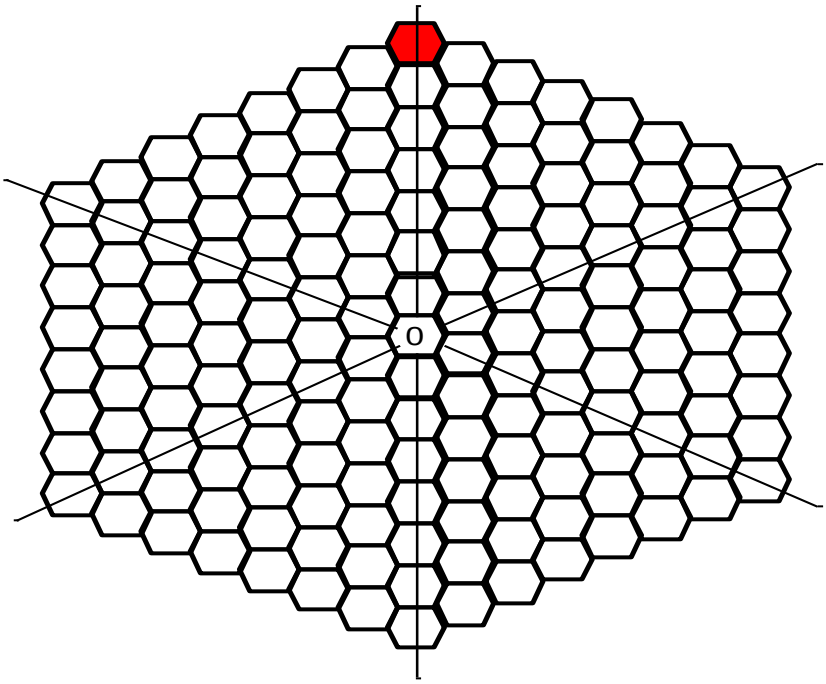

Figure 3.2 The cell pattern with the red marked interfering cell (shift parameters i=7 and j=0)

Next, the indicator i is reduced to one and it becomes six, and the indicator j will take the values zero and one, see Figure 3.3

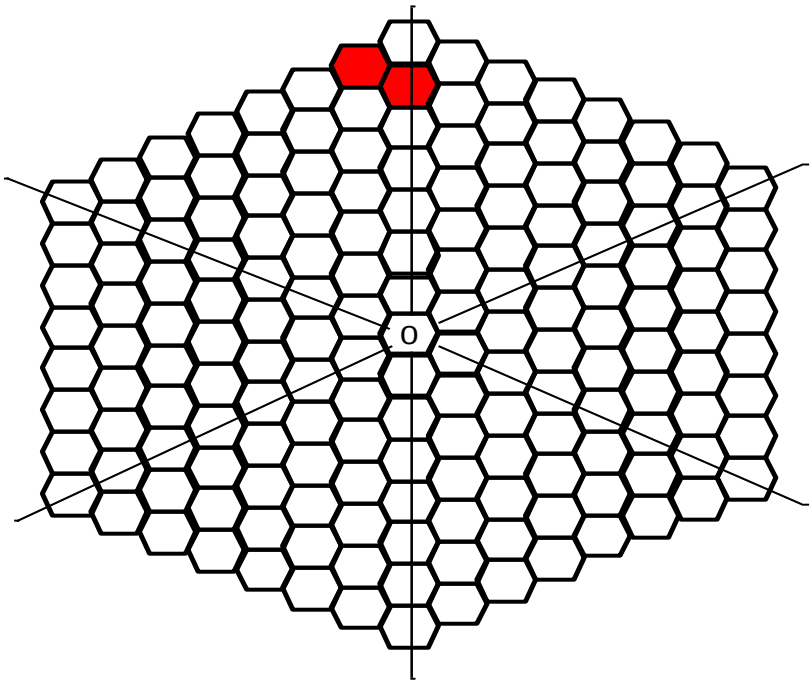

Figure 3.3 The cells pattern with the red marked interfering cells (shift parameters i=6 and j=1)

Next, the indicator i is reduced to one and it becomes five, and the indicator j will take values zero, one and two, see Figure 3.4.

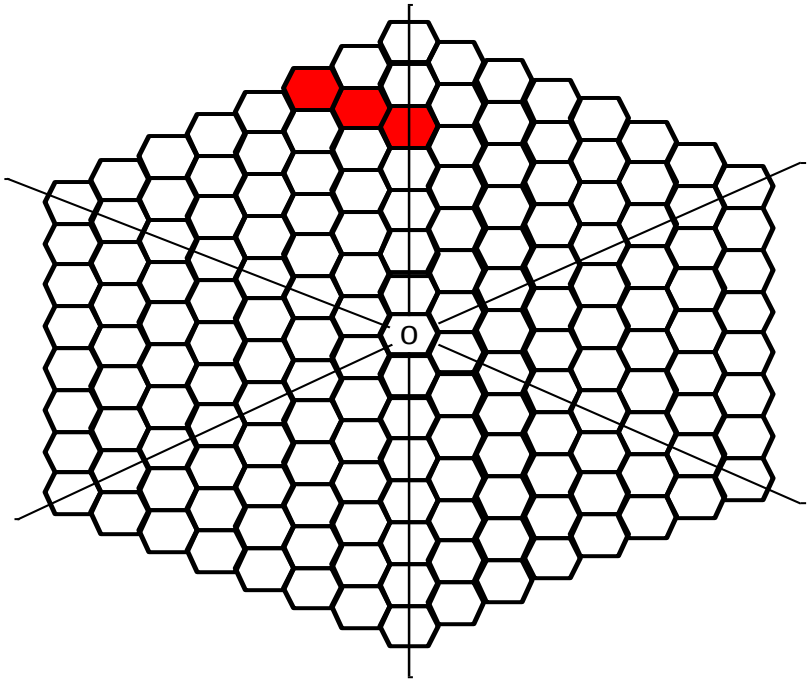

Figure 3.4 The cells pattern with the red marked interfering cells (shift parameters i=5 and j=0,1,2)

The indicator i is reduced with the same logic each time by one and it ends up in its final price which is one and the indicator j will take the values 0, 1, 2, 3, 4, 5 and 6, see Figure 3.5

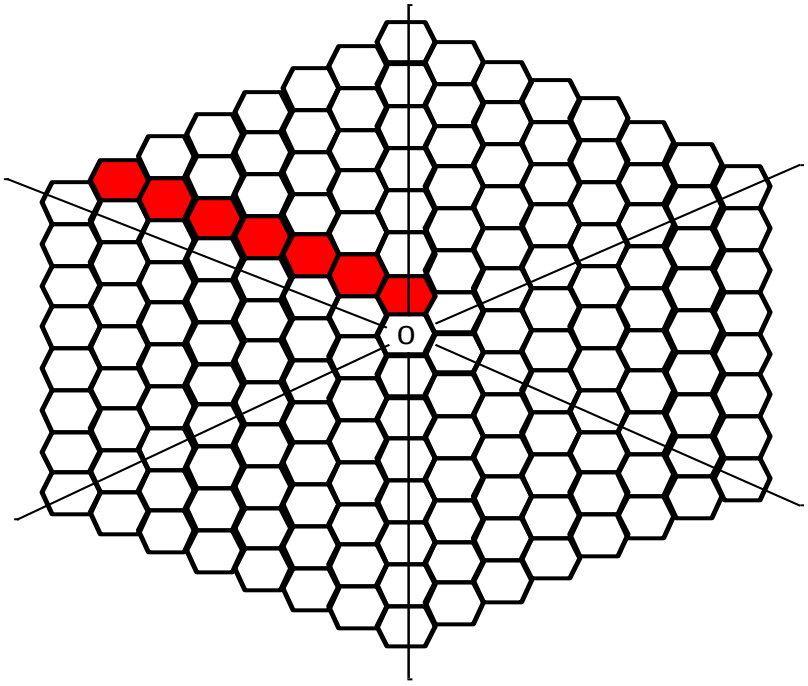

Figure 3.5 The cells pattern with the red marked interfering cells (shift parameters i=1 and j=0,1,2,3,4,5,6)

It is obvious that in order to take the final value of f_R, it is enough to multiply triple integral by six, because for each cell in the mentioned sector, there are five similar interfering cells, one in each sector, in the other five sectors.

In this way scanning the 28 (=168/6) cells of one sector, we have added in essence all the interfering cells.

Table 3.1 Part of the code in Matlab

for i=7:-1:1
for j=0:1:(7-i)
Di=1.732*sqrt((i*R+0.5*j*R)^2+(0.866*j*R)^2);
yi=(i+j/2)*1.732*R; % i coordinate y of the position of each cell
xi=sqrt(Di.^2-yi.^2); % i coordinate y of the position of each cell, is calculated with the use of the Pythagorean Fundamental
Di^2=xi^2+yi^2
fRi=@(r,phi,z)(((Di.^2+r.^2+z.^2+2.*r.*(xi.*cos(phi)+yi.*sin(phi))).^-1).*p.*(z.^2+r.^2).*r.*myfun(r,phi,xi,yi,Di,z
% the integration function as in the paper, we define that the variables of the function are r, f (ankle) and z, function my fun constitutes the indicator function, namely eliminates f for R>RLOS
fR=6*triplequad(fRi,0,R,0,2*pi,0,h);
fRi_i=fRi_i+fR;
End
End

In the same logic we do the scanning of the interfering cells for f_F .

So that the same calculations don't have to be carried out, we replace the values which don't change, outside the variable z, and we have the Radio Line of Sight as a function of z

$$\mathrm{RLOS}(z) = \sqrt{\frac{(2 \cdot 4)\mathrm{r_e}}{3}}\sqrt{\mathrm{z}} = 3{,}366.502\,\sqrt{\mathrm{z}} = 3{,}366.502 \cdot \sqrt{\mathrm{z}}$$

3.3 Results for the f_R

In order to calculate OCIF f_R we used the equations (2.12), (2.11), (2.11a) and (2.21) also having in mind the Matolak's model, Figure 2.2.b. Using my algorithm described in section 3.2, and the part of Matlab code of Table 3.1, the OCIF is calculated for every interfering cell, for the pair of values (R,h) where R is the cell radius and h is the maximum height of the cell. R and h values are chosen to be the same as in Figure 2 in [2] for comparison. Matolak in [2] do not provide details for his algorithm but he gives the values of R and h.

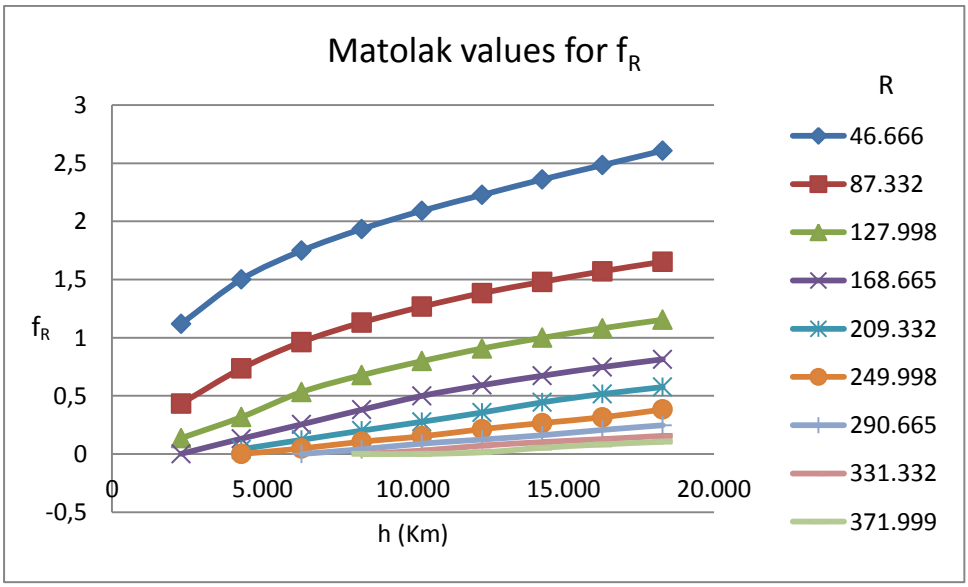

Figure 3.6 The values of f_R, each curve is for different R (R=46.666 km, R=87.332 km, R=127.998 km, R=168.665 km, R=209.332 km, R=249.998 km, R=290.665 km, R=331.332 km and R=371.999 km), and for h=2.3 km, h=4.3 km, h=6.3 km, h=8.3 km, h=10.3 km, h=12.3 km, h=14.3 km, h=16.3 km and h=18.3 km.

Below the same results can be seen in the form of a table, namely the value of f_R for each pair of values of the (R, h). In the first line there are the different values of h, while in the first column there are the values of R.

h(km) / R(km)	2.300	4.300	6.300	8.300	10.300	12.300	14.300	16.300	18.300
46.666	1.119	1.502	1.748	1.934	2.091	2.227	2.361	2.484	2.608
87.332	0.433	0.735	0.963	1.131	1.266	1.383	1.480	1.571	1.653
127.998	0.136	0.317	0.533	0.678	0.798	0.907	0.999	1.081	1.154
168.665	0.002	0.132	0.255	0.381	0.500	0.592	0.673	0.748	0.814
209.332		0.041	0.122	0.201	0.277	0.357	0.444	0.516	0.575
249.998		0	0.048	0.106	0.152	0.214	0.266	0.316	0.382
290.665			0	0.042	0.089	0.124	0.161	0.207	0.247
331.332				0	0.029	0.072	0.102	0.128	0.156
371.999				0	0	0.015	0.053	0.082	0.105

Table 3.2 The values of f_R for each pair of values of (R, h).

If we compare the f_R to our results for values R=168.66 km and h = 12.3 km, which are close to the values of the case study for Greece, it can be observed that it is 0.592 which is similar to Figure 2 of Matolak [2].

The same simulations setups are valid also in Figure 3.7, which compares the proposed results for f_R that are computed from our algorithm, with those of Smida [4, Figure 5], using now the same values of R and h with Smida [4] for comparison. In [4] upper and lower bounds, as well as the actual value for OCIF are provided using close form equation [equation (19) in 4].

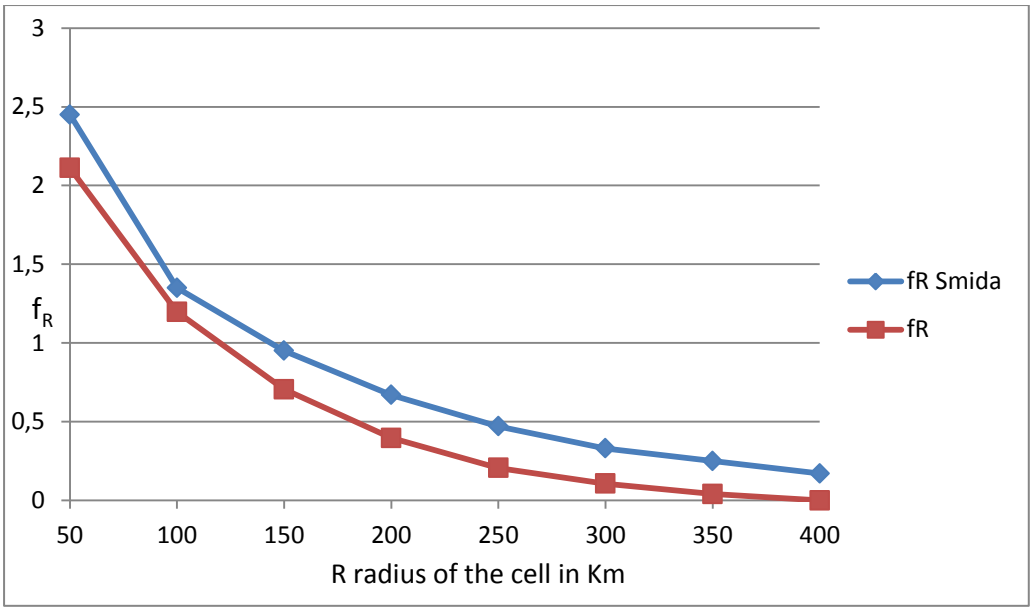

Figure 3.7 Values of f_R, for R=50 km, R=75 km, R=100 km, R=125 km, R=150 km, R=175 km, R=200 km, R=225 km, R=250 km, R=275 km, R=300 km, R=350 km and R=400 km and h = 12 km.

Having some slight deviations in the numerical calculations among the researchers due to some accuracy errors and different outputs is considered logical.

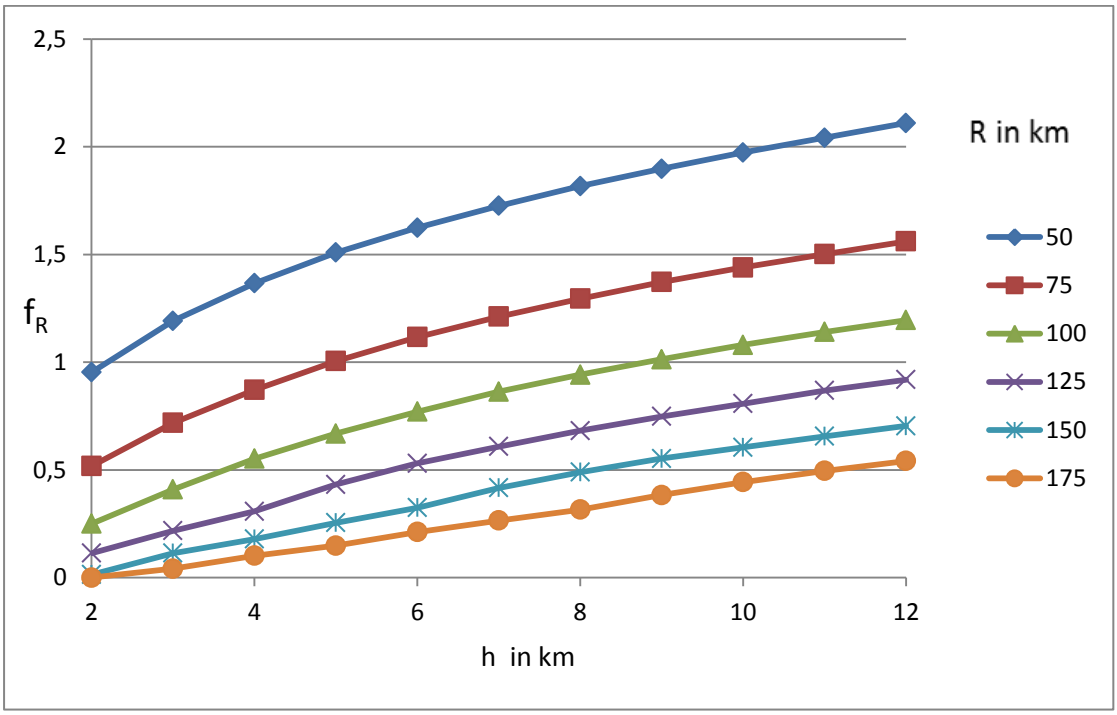

Figure 3.8.1 The f_R as a function of h up to12 km (step 1 km) . Each curve is for a specific value of R=50 km, R=75 km, R=100 km, R=125 km, R=150 km and R=175km.

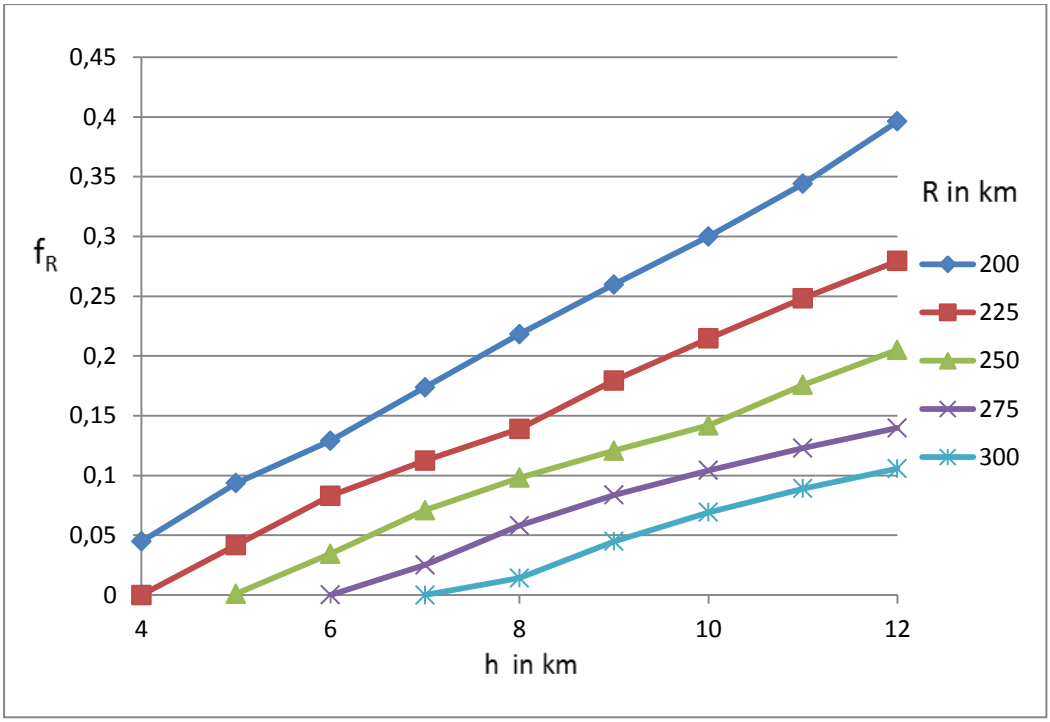

Figure 3.8.2 The f_R as a function of h up to12 km (step 1 km) . Each curve is for a specific value of R=200 km, R=225 km, R=250 km, R=275 km and R=300 km.

3.4 Results for f_F

$\mu_i = f_{Fi}(h, R)$ is calculated using Matlab employing equations (2.53a) and (2.11a) for different values of R and h for each interfering cell. The scanning of 168 cells is done in the same way as it has been previously explained in the algorithm of the calculation of f_R.

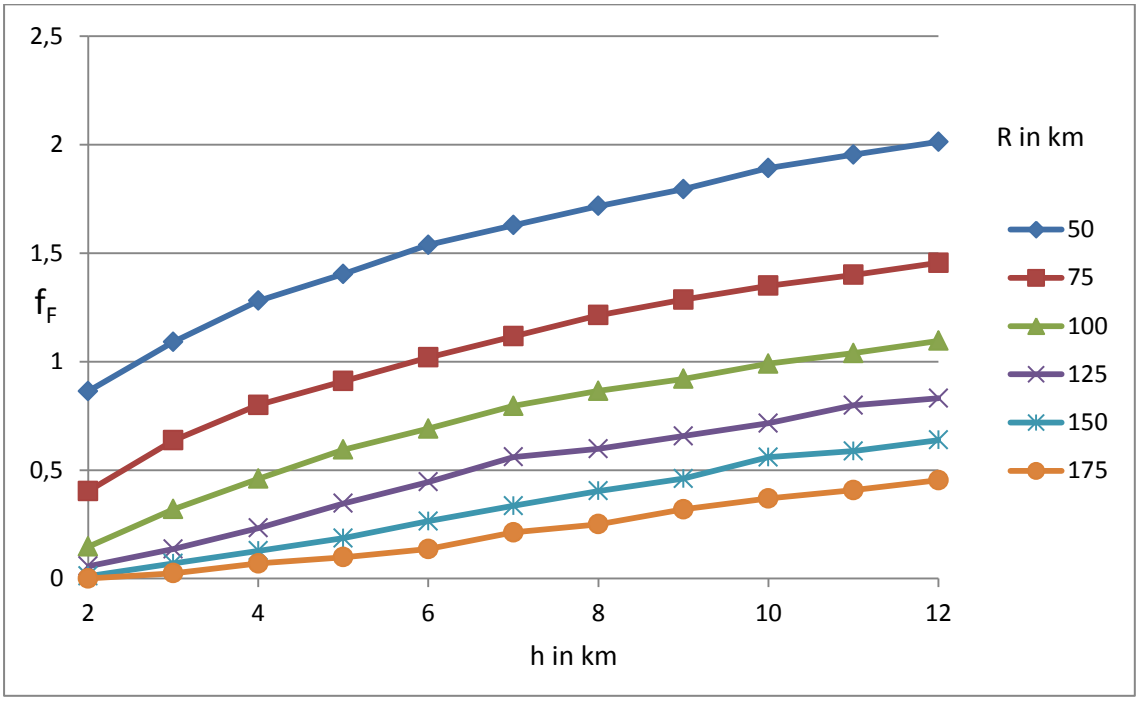

Figure 3.9.1 The f_F as a function of h up to12 km (step 1 km). Each curve is for a specific value of R=50 km, R=75 km, R=100 km, R=125 km, R=150 km and R=175km.

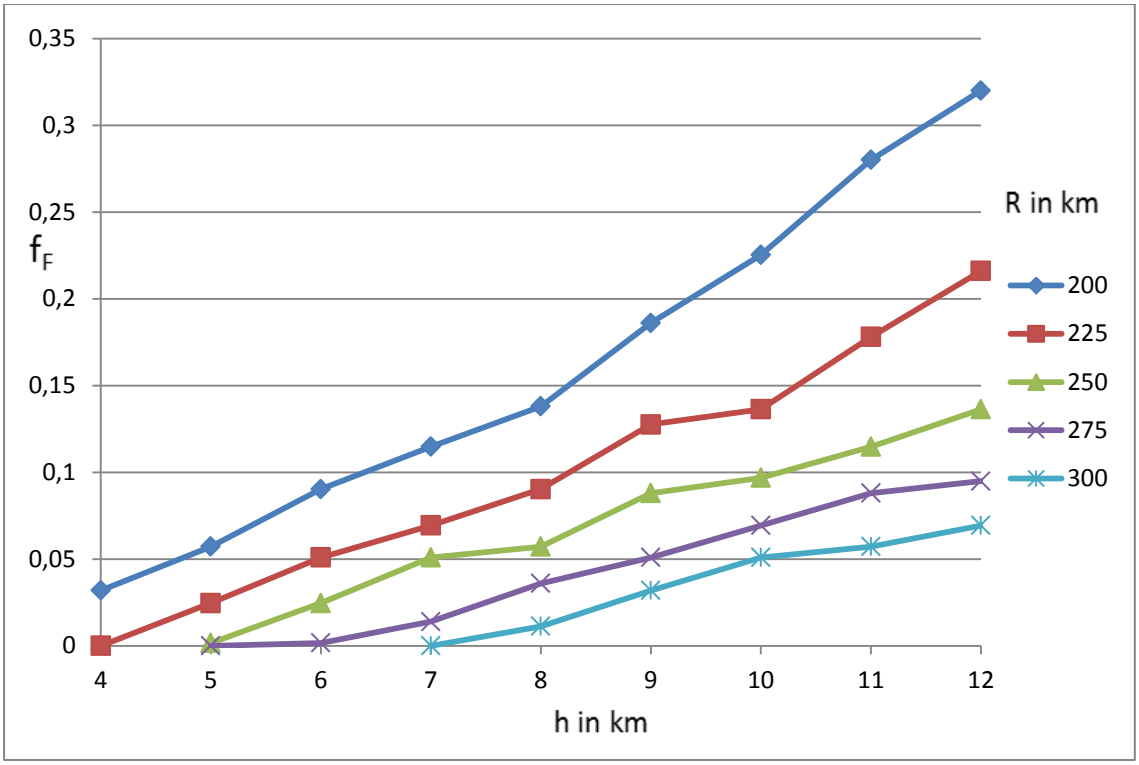

Figure 3.9.2 The f_F as a function of h up to12 km (step 1 km). Each curve is for a specific value of R=200 km, R=225 km, R=250 km, R=275 km and R=300 km.

3.5 Calculation of the number of subscribers

Number M of the subscribers will be calculated for h, which is the height of the cell for different values of R both for forward and for reverse link, and the minimum M will be derived. In this way it will be found, which of the two links determines the capacity of the cell.

So there will be

W = 3.84 Mcps WCDMA chip rate

R_b bit rate of user = 12.2 kbps, because it is assumed that all the subscribers will have only voice service.

3.6 Reverse link

From the relationship (2.30) and by using $n_{UL} = 0.9$, M in the reverse link will become:

$$M = \frac{3 \cdot \left(\frac{3840\ \text{kbps}}{12.2\ \text{kbps}}\right) \cdot \frac{1}{0.545}}{5.012} \cdot n_{UL} \cdot \frac{1}{1 + f_R} = 311.1198 \cdot \frac{1}{1 + f_R}$$

Therefore

$$M = 311.1198 \cdot \frac{1}{1 + f_R}$$

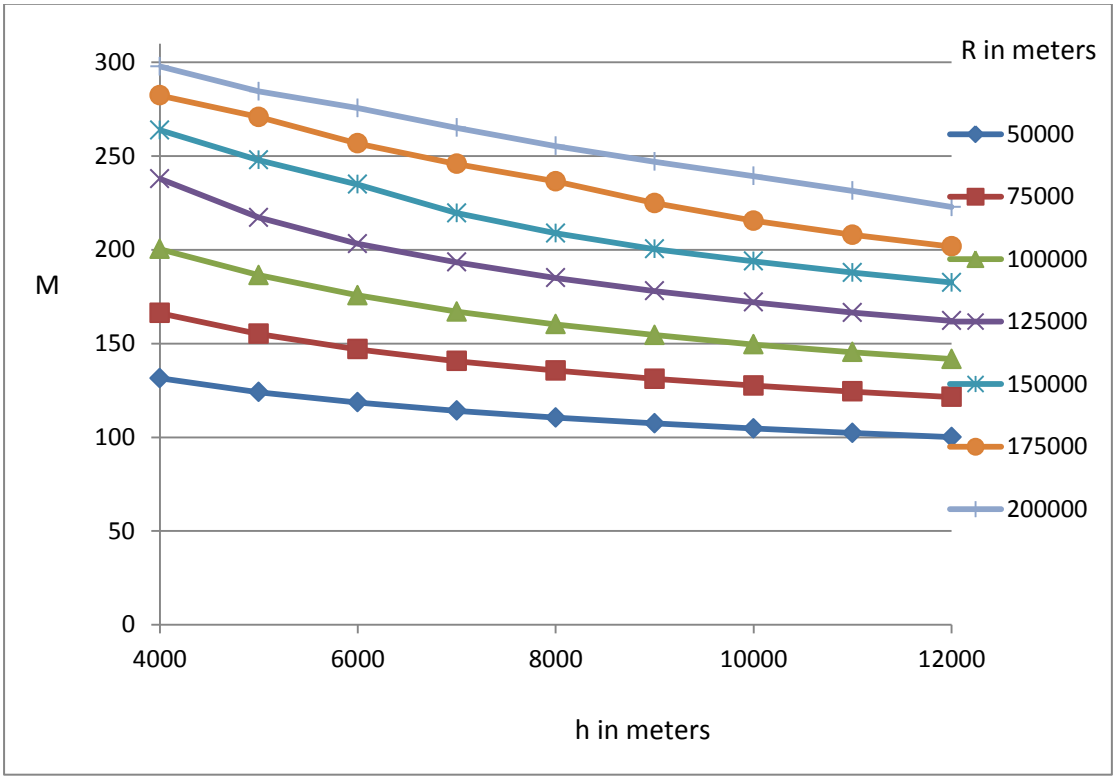

Figure 3.3.1 M voice users in Reverse link, $R_b = 12.2$Kbps, W=3.84Mcps, activity factor v=0.545, $n_{UL} = 0.9$, $\frac{E_b}{N_o} = 7$ dB, for R=50 km, R=75 km, R=100 km, R=125 km, R=150 km, R=175 km, R=200 km and for various values of h starting from 4 km to 12 km (step 1 km).

R \ h	4000	5000	6000	7000	8000	9000	10000	11000	12000
50000	131	123	118	114	110	107	104	102	100
75000	166	155	146	140	135	131	127	124	121
100000	200	186	175	166	160	154	149	145	141
125000	237	217	203	193	184	177	172	166	162
150000	263	247	234	219	208	200	193	187	182
175000	282	270	256	245	236	224	215	207	201
200000	297	284	275	265	255	246	239	231	222

Table 3.3 M voice users in Reverse link, $R_b = 12.2$Kbps, W=3.84Mcps, activity factor v=0.545, $n_{UL} = 0.9$, $\frac{E_b}{N_o} = 7$ dB, for R=50, 75, 100, 125, 150, 175, 200 km and for various values of h starting from 4 km to 12 km (step 1 km).

3.7 Forward link

In order to calculate the capacity in the forward link, the values in Table 4.3 E_b/N_o are used, which are derived from the respective values for the terrestrial systems from [8], Table 11.21, by adding 2dB due to the Air-to-Ground model , as explained in [11].

Therefore, $\frac{E_b}{N_o} = 6.4 + 2 = 8.4$ dB.

Transforming dB to a net number,

$10 \log_{10}\left(\frac{E_b}{N_o}\right) \underset{net\ value}{\Longrightarrow} = 8.4$dB

The $\left(\frac{E_b}{N_o}\right)_{net\ value} = 6.9183097092$

To activity factor is $\frac{3}{8} + 0.17$ DCCM overhead $= 0.375 + 0.17 = 0.545$.

From the relationship (2.43) and using $n_{DL} = 0.9$, M in the forward link will become:

$$M = \frac{3 \cdot \left(\frac{3840\ \text{kbps}}{12.2\ \text{kbps}}\right) \cdot \frac{1}{0.545}}{5.012} \cdot n_{DL} \cdot \frac{1}{f_F} = 311.1198 \cdot \frac{1}{f_F}$$

Therefore

$$M = 311.1198 \cdot \frac{1}{f_F}$$

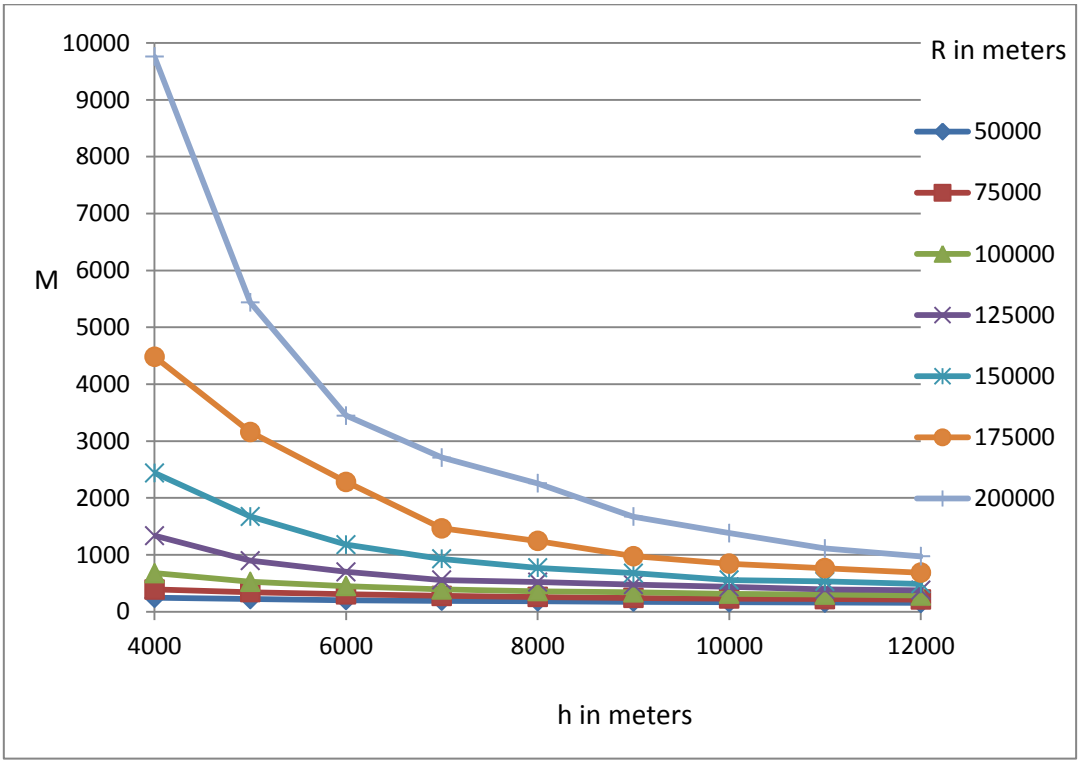

Figure 3.3.2 M voice users in Forward link, $R_b = 12.2$Kbps, W=3.84Mcps, activity factor v=0.545, $n_{DL} = 0.9$, $\frac{E_b}{N_o} = 7$ dB, for R=50 km, R=75 km, R=100 km, R=125 km, R=150 km, R=175 km, R=200 km and for various values of h starting from 4 km to 12 km (step 1 km).

R \ h	4000	5000	6000	7000	8000	9000	10000	11000	12000
50000	242	221	202	191	181	173	164	159	154
75000	388	341	305	278	256	242	230	222	213
100000	676	523	450	391	359	338	314	299	283
125000	1336	897	699	555	520	473	434	389	374
150000	2438	1672	1177	927	771	675	556	529	487
175000	4483	3158	2281	1464	1242	975	842	762	686
200000	9759	5439	3445	2710	2255	1672	1380	1110	972

Table 3.4 M voice users in Forward link, $R_b = 12.2\text{Kbps}$, W=3.84Mcps, activity factor v=0.545, $n_{DL} = 0.9$, $\frac{E_b}{N_o} = 7$ dB, for R=50 km, R=75 km, R=100 km, R=125 km, R=150 km, R=175 km, R=200 km and for various values of h starting from 4 km to 12 km (step 1 km).

By comparing tables 3.3 and 3.4 it can be seen that the limitation in the capacity is set by the reverse link, where the number of subscribers is significantly smaller. Therefore the values from table 3.3 will be used for the capacity of the Air Ground system.

3.8 Summary

The algorithm used to calculate the OCIF has been explained for both links and its results are given for different values of height and radius of the cell. Moreover, the numerical values for the capacity per cell were calculated for different values of the height and the radius of the cell.

Chapter4: Case study for Greek Airports

4.1 Introduction

In this chapter we are studying three scenarios for the capacity of an Air-to-Ground system for Greek Airports where the base stations are located at the airports.

4.2 Scenario 1

The first scenario includes the three major airports in Greece, the Eleftherios Venizelos Airport of Athens, the Macedonia Airport of Thessalonica and the Nick Kazantzakis Airport of Heraklion.

The web site Airport Distance Calculator [15] will be used in order to calculate the distance between the two airports. From this, the distance between the Eleftherios Venizelos Airport of Athens (ATH) and the Nick Kazantzakis Airport of Heraklion (HER) is 308.65km. The distance between the Eleftherios Venizelos Airport of Athens (ATH) and the Macedonia Airport of Thessalonica (SKG) is 299. 49 km.

Based on the above distances the size of the cells will be R= 175km, so setting a cell centered at Athens and another centered at Heraklion will cover 2X175 =350 km and there is also overlapping so that the handover can be plausible.

The maximum height of the cell is chosen to be h=12000m or almost 39344 feet, because commercial flights fly between the 25000 and 39000 feet [16-18]. In this way by choosing the height of the cellular cell to be h=12000m all the possible heights of commercial flights are included.

Three sectors will be used for every site (base station) so that the coverage can simulate in the cellular model we have used for the calculation of the OCIF. The directions of the antennas will be per 120^{o}. In Athens we will have the antenna pointing directions 50, 170 and 290 degrees. Thessalonica will have the same directions as Athens.

In the bisector of the directions of the sectors e.g. between the 170 degrees direction and 290 degrees direction, namely 230 degrees (bisector), where there will be the maximum attenuation, which for the typical antenna pattern there will be almost -9dB attenuation in relation to the maximum value. So, it will be assumed for simplicity that the signal level will be almost stable in the perimeter of the cellular

cell. In fact, the interference which can be found in our calculations is higher as it has been assumed that the maximum value in the periphery of the circular cell – cylindrical cell.

In Figure 4.1 the map of Greece is illustrated showing the three airports of the first scenario along with the directions of the sectors and their base stations. In the radio-coverage charts of terrestrial mobile telecommunication systems, the focus is on land coverage and it is obvious the shadowing effect of electromagnetic radiation due to the morphology of earth's surface. Unlike this, in the Air-to-Ground system because the beams of the antennas aim high at the aircrafts, the electromagnetic shading which may exist in the low altitudes is not depicted, but the coverage appears at the height the aircrafts fly. In Figure 4.1 the range of the 175km is depicted in the direction of the sector and the total form of the coverage of each base station, it derives from the combination of the three radiation charts of the sectors. The final form of the coverage of the base station approaches the cylindrical structure of the cells.

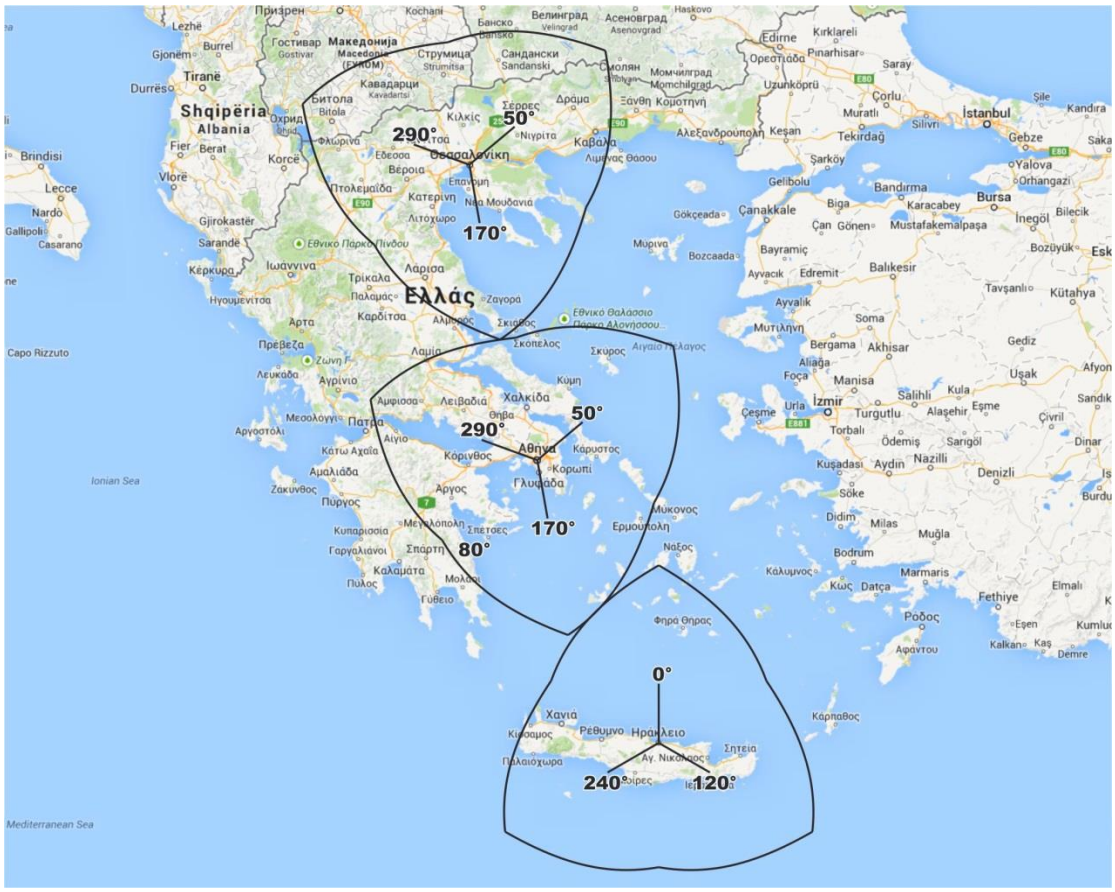

Figure 4.1 Map of Scenario 1, R=175km, h=12 km.

Table 4.1 summarizes the scenario 1

				Distances between Airports in km	
	Base Stations	Antenna Sectors, Directions in degrees	R in km	Thessaloniki	Heraklio
1	Athens (ATH)	50, 170, 290	175	299	309
2	Thessaloniki (SKG)	50, 170, 290	175		608
3	Heraklio (HER)	0, 120, 240	175		

Table 4.1 Scenario 1: 3 Base Stations (BS) with one cell per BS and 9 sectors.

4.3 Scenario 2

The 2nd scenario could be the second stage of implementation which will succeed the first stage, which is depicted in scenario 1, as the Air-to-Ground network will grow. In this scenario we retain the same range of cells in which R = 175 km and the same maximum flying height which is h = 12 km, which is the height of the cellular cell. We add three new airports the airports of Rhodes, Corfu and Mytilene in order to cover almost all of Greek airspace. In Figure 4.2 the cells of the scenario 2 are depicted with the directions of the sectors and the outlines of their ranges. Table 4.2 shows the details of scenario 2.

Figure 4.2 Map of Scenario 2, R = 175 km, h = 12 km

				Distances between Airports in Km				
	Base Stations	Antenna Sectors, Directions in degrees	R	Thessaloniki	Heraklio	Rhodes	Corfu	Mytilene
1	Athens (ATH)	50, 170, 290	175km	299	309	404	396	262
2	Thessaloniki (SKG)	50, 170, 290	175km		608	638	280	350
3	Heraklio (HER)	0, 120, 240	175km			287	664	432
4	Rhodes (RHO)	60, 180, 300	175km				799	323
5	Corfu (CFU)	0, 120, 240	175km					578
6	Mytilene (MJT)	50, 170, 290	175km					

Table 4.2 Scenario 2: 6 Base Stations (BS) with one cell per BS and 18 sectors.

It is quite interesting to see further the results of the simulations for the capacity of each cell, namely the number of users M, as a function of the bit rate R_b for voice and packet data. Figure 4.3 which is valid for both scenario 1 and scenario 2, where R = 175 km and the h = 12 km. In order to calculate the capacity in the forward link, E_b/N_o values in Table 4.3 are used, which were derived from the corresponding values for the terrestrial systems as depicted in [8], Table 11.21, adding 2dB because of the Air-to-Ground model. As n_{DL} the value of 0.9 is being used everywhere.

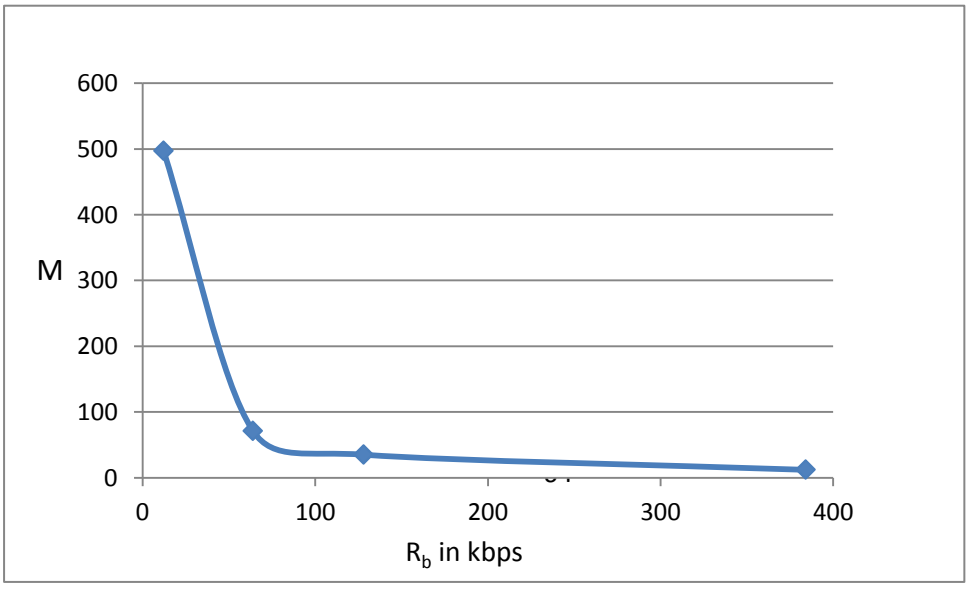

Figure 4.3: The number of users M for the forward link, as a function of the bit rate R_b for voice and packet data for R = 175 km, h = 12 km and $n_{DL} = 0.9$.

Table 4.3: The number of users M for the forward link, as a function of the bit rate R_b for voice and packet data, for R=175 km, h = 12 km and n_{DL}=0.9. In case of the voice service the activity factor is v=3/8+0.17 DPCCH overhead=0.375+0.17=0.545, while in the only data case it is v=1.

Eb/No	6.92	5.01	5.01	4.90
Eb/No in dB	8.4	7	7	6.9
Rb (in kbps)	12.2	64	128	384
M	497	71	35	12

In order to calculate the capacity in the reverse link, E_b/N_o values in Table 4.4 are used as before. By comparing Tables 4.3 and 4.4 we can notice that the limitation of the system capacity for the case of the voice or the video call service which requires symmetrical traffic in both links, is taken by the reverse link, because this is where the lowest capacity exists. Therefore, the final capacity of the Air-to-Ground system is similar to the capacity of the reverse link, Figure 4.4. and Tables 4.4 and 4.5. In Table 4.5 the number of users per cell and full capacity is presented for scenario 1 and 2 for voice call 12.2 kbps and video call services of 64 kbps and 128 kbps , which all concern symmetric traffic. The capacity of the cell is determined by the lowest value of the users for DL and UL. In case of data service there is no symmetric traffic because usually the forward link has significantly greater traffic from the reverse link. Hence, it can be assumed that in the data services there will be the following three types of users:

1. 64 kbps in the DL and 12.2 kbps in the UL,
2. 128 kbps in the DL and 64 kbps in the UL,
3. 384 kbps in the DL and 128 kbps in the UL.

Table 4.6 presents the number of users per cell and the full capacity is presented for this case. For n_{UL} and n_{DL} 0.9 is always used. In Table 4.6, for data service 12.2kbps in the UL, there are 98 users, while in Table 4.5, for voice service of 12.2 kbps in the UL, there are 179 users. This difference is due to the fact that in Table 4.6, for data service, the activity factor is 1, while in Table 4.5 the voice service the activity factor is 0.545.

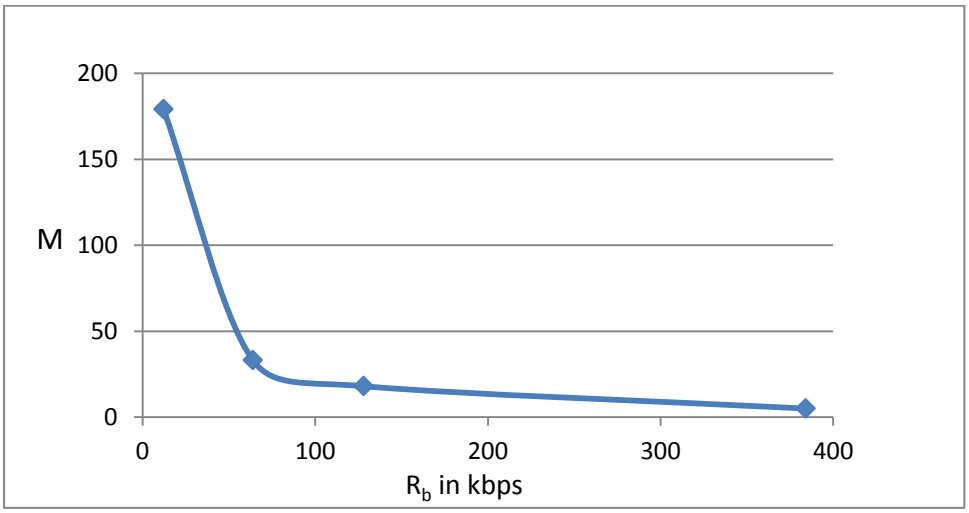

Figure 4.4: The number of users M for the reverse link, as a function of the bit rate R_b for packet data for R = 175 km, h = 12 km and $n_{UL} = 0.9$.

E_b/N_o	5.62	3.16	2.81	3.16
E_b/N_o (in dB)	7.5	5	4,5	5
R_b (in kbps)	12.2 (voice)	64	128	384
M users per cell	179	33	18	5

Table 4.4: The number of users M for the reverse link, as a function of the bit rate R_b for packet data for R = 175 km, h = 12 km and $n_{UL} = 0.9$.

Services	Voice call	Video call	
R_b (in kbps) for both DL and UL	12.2	64	128
M users per cell for DL	497	71	35
M users per cell for UL	179	33	18
M users per cell (min value from DL and UL)	179	33	18
Total users scenario 1	537	99	54
Total users scenario 2	1074	198	108

Table 4.5: The number of users M for voice call and video call services – symmetric traffic, as a function of the bit rate R_b for DL and UL, for R = 175 km, h = 12 km, $n_{UL} = 0.9$ and $n_{DL} = 0.9$.

Services	data	data	data
R_b (in kbps)	64DL, 12.2UL	128DL, 64UL	384DL, 128UL
M users per cell for DL	71	35	12
M users per cell for UL	98	33	18
M users per cell (min value from DL and UL)	71	33	12
Total users scenario 1	213	99	36
Total users scenario 2	426	198	72

Table 4.6: The number of users M for data services– asymmetric traffic, as a function of the bit rate R_b for DL and UL, for R = 175 km, h = 12 km, $n_{UL} = 0.9$ and $n_{DL} = 0.9$.

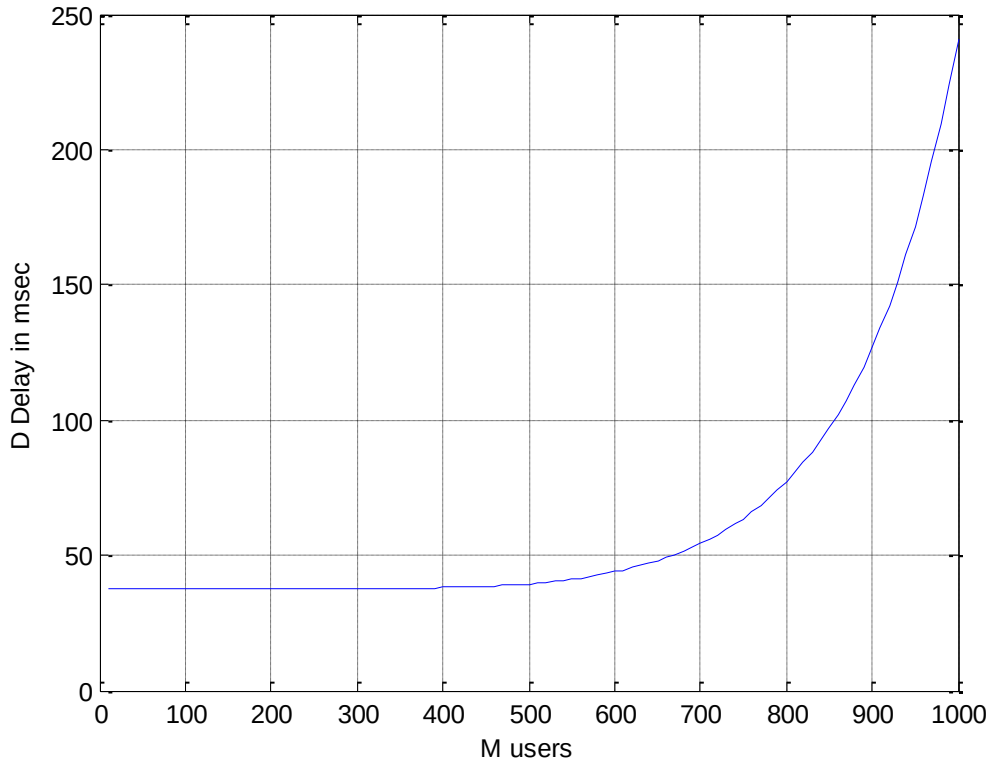

Figure 4.5: Delay D as a function of the number of users for the forward link, $R_b = 12.2$ kbps (bit rate) for voice, for R = 175 km and h = 12 km, the activity factor is v = 0.545, packet length L = 424bits, $t_d = 3$ msec and $n_{DL} = 0.9$.

Figure 4.5 shows the delay D for voice service $R_b = 12.2$ kbps using equation (2.67) as a function of the number of users for the forward link. We take the transmission time and procession $t_d = 3$ ms [3, 1]. Hence for scenarios 1 and 2 the delay is, D =37.7541ms, for M=179 users per cell (see Table 4.4) which is the capacity defined by the Reverse link.

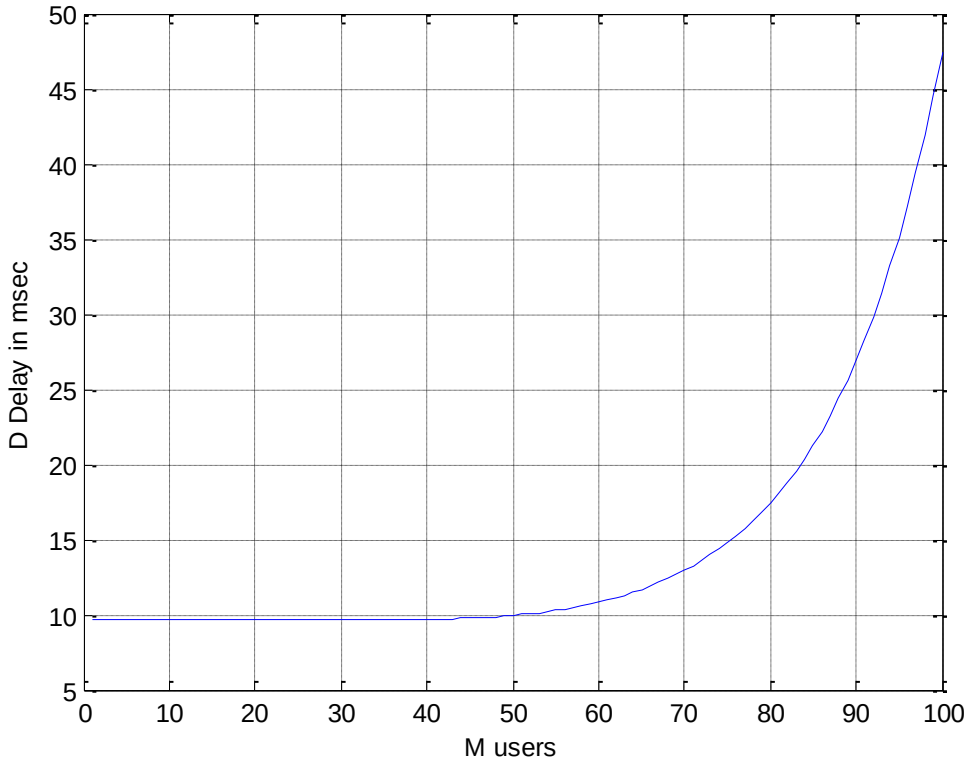

Figure 4.6: Delay D as a function of the number of users for the forward link, $R_b = 64$ kbps (bit rate) for data, for R = 175 km and h = 12 km, the activity factor is v = 1, packet length L = 424bits, $t_d = 3$ msec and $n_{DL} = 0.9$.

Figure 4.6 shows delay D for data service $R_b = 64$ kbps. Therefore for scenarios 1 and 2 the delay for the symmetric traffic will be D = 9.6317msec, for M = 33 users per cell (see Table 4.5), while for asymmetric traffic (see Table 4.6), data service 64 DL & 12.2 UL will increase the delay to 13.2602 msec, if the users become 71.

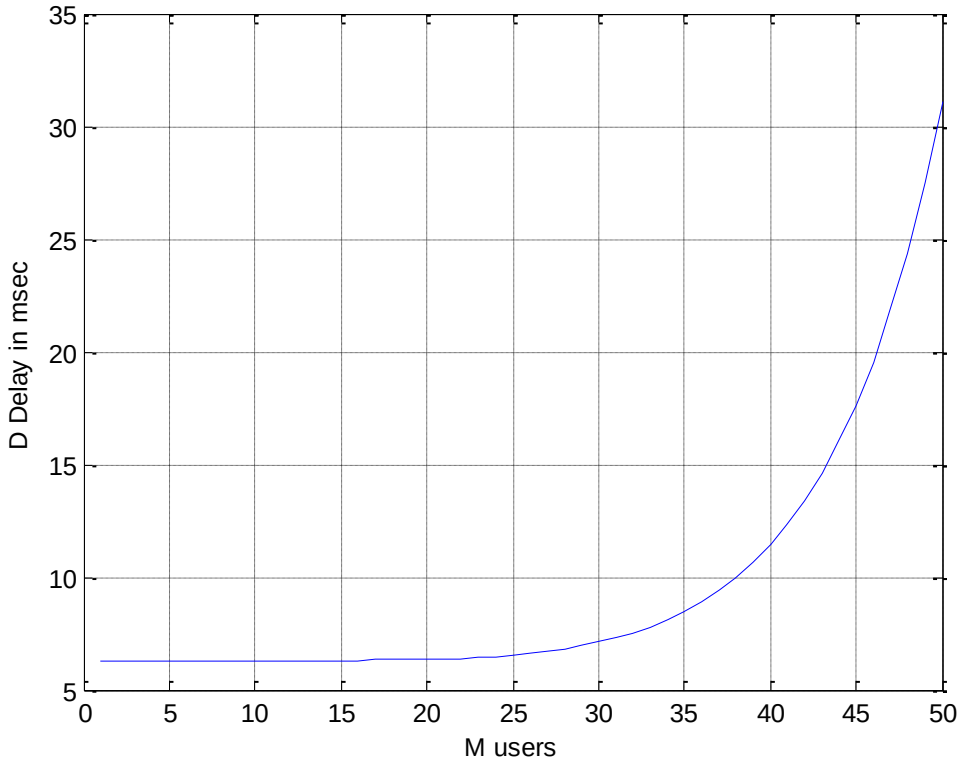

Figure 4.7: Delay D as a function of the number of users for the forward link, $R_b = 128$ kbps (bit rate) for data, for R = 175 km and h = 12 km, the activity factor is v = 1, packet length L = 424bits, $t_d = 3$ msec and $n_{DL} = 0.9$.

Figure 4.7 shows delay D for data service $R_b = 128$ kbps. Therefore for scenarios 1 and 2 the delay for symmetric traffic, will be D = 6.3237 msec, for M = 18 users per cell (see Table 4.5), while for asymmetric traffic (see Table 4.6), data service 128 DL & 64 UL the delay will increase to 7.8032 msec, if the users become 33.

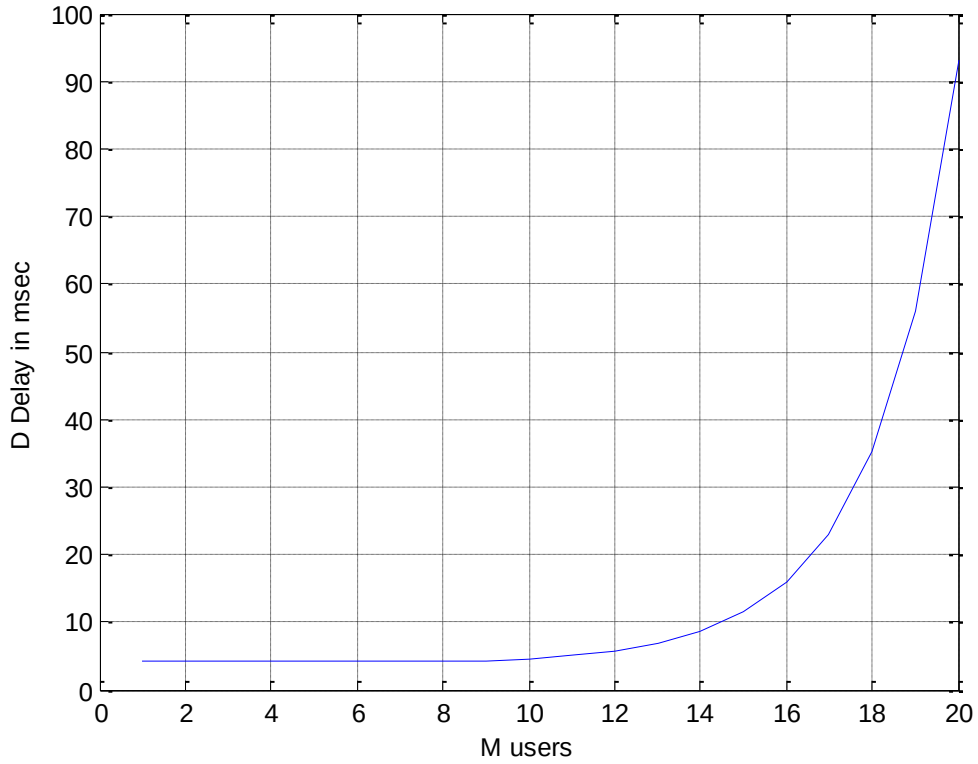

Figure 4.8: Delay D as a function of the number of users for the forward link, $R_b = 384$ kbps (bit rate) for data, for R = 175 km and h = 12 km, the activity factor is v = 1, packet length L = 424 bits, $t_d = 3$ msec and $n_{DL} = 0.9$.

Figure 4.8 shows delay D for data service $R_b = 384$ kbps. Therefore for scenarios 1 and 2 the delay for symmetrical traffic will be D = 4.1051msec, for M = 5 users per cell (see Table 4.5), while for asymmetric traffic (see Table 4.6), data service 384 DL & 128 UL the delay will increase to 5.7990 msec, if the users become 12.

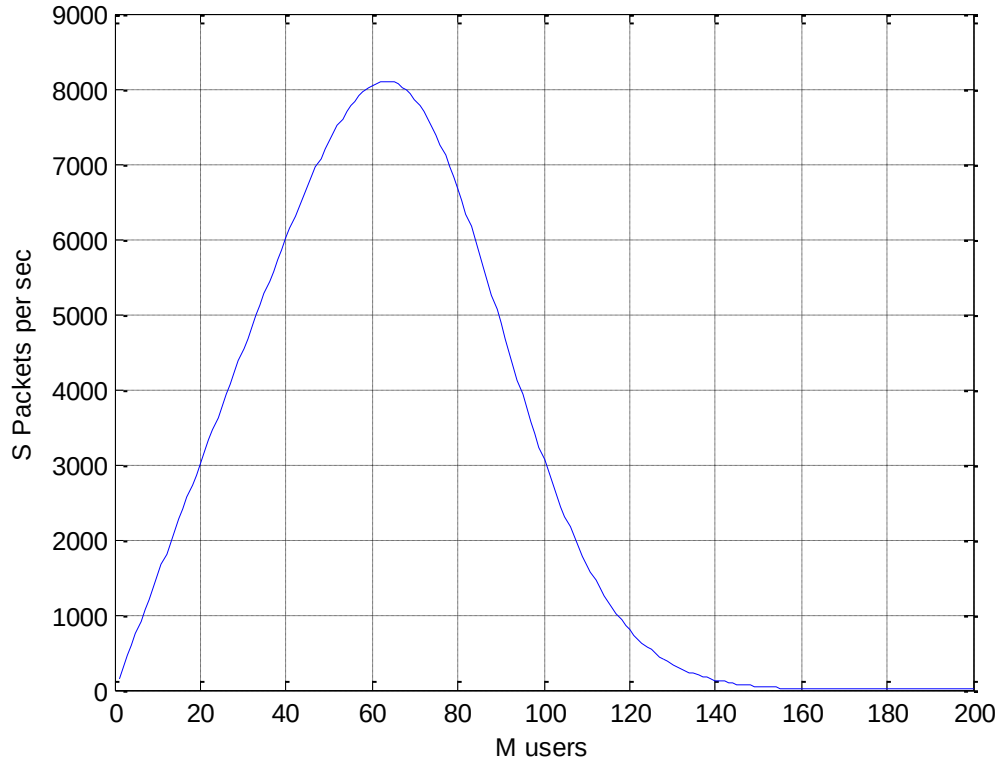

Figure 4.9: Throughput in packets per second as a function of the number of users for the forward link, $R_b = 64$ kbps (bit rate) for data, for R = 175 km and h = 12 km, the activity factor is v = 1, packet length L = 424 bits and $n_{DL} = 0.9$.

Throughput is calculated using equation (2.68). As it can been seen in Figure 4.9, the maximum throughput for symmetric traffic for video cell (Table 4.5), at 64 kbps is at M = 63 with 8099 packets per second, however, due to the reverse link the capacity is limited to 33 users and the throughput is 4977 packets per sec. In the case of the asymmetric traffic (Table 4.6) the maximum value of the throughput is exploited, 8099 packets per second, for 63 users, because the maximum number of users in the data service 64 DL& 12.2 UL, is 71.

As it is obvious in Figure 4.10, the throughput for the symmetric traffic of the video call (see Table 4.5), in the 128 kbps it would take its maximum value for M = 32 users and it would become 8096 packets per sec, however, due to the reverse link the capacity is limited to18 users and the throughput is 5424 packets per sec. In the case of the asymmetric traffic (see Table 4.6), the maximum value of the throughput is

exploited 8096 packets per sec, for 32 users, because the maximum number of users in the data service 128 DL & 64 UL, is 33.

As can be seen in Figure 4.11 the throughput in the 384kbps where we have only asymmetric traffic (see Table 4.6), the maximum value of the throughput is exploited, 8059 packets per sec, for 11 users, because the maximum number of users in the data service 384 DL & 128 UL, is 12.

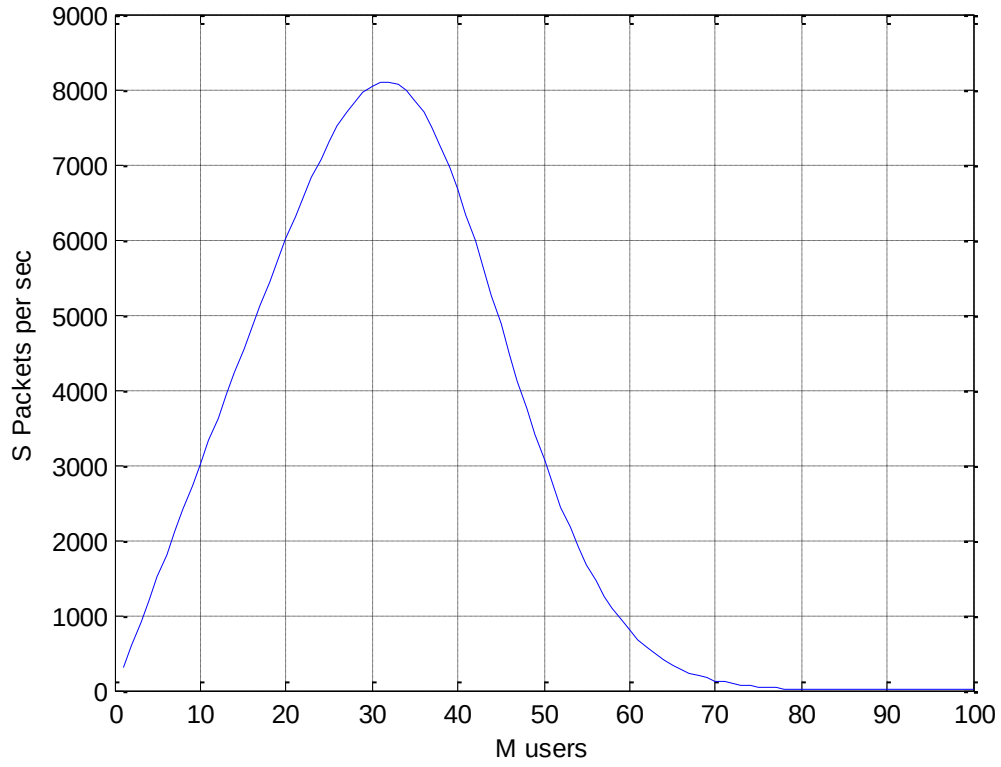

Figure 4.10 Throughput in packets per sec as a function of the number of users for the forward link, $R_b = 128$ kbps (bit rate) for data, for R = 175 km and h = 12 km, the activity factor is v = 1, packet length L = 424 bits and $n_{DL} = 0.9$.

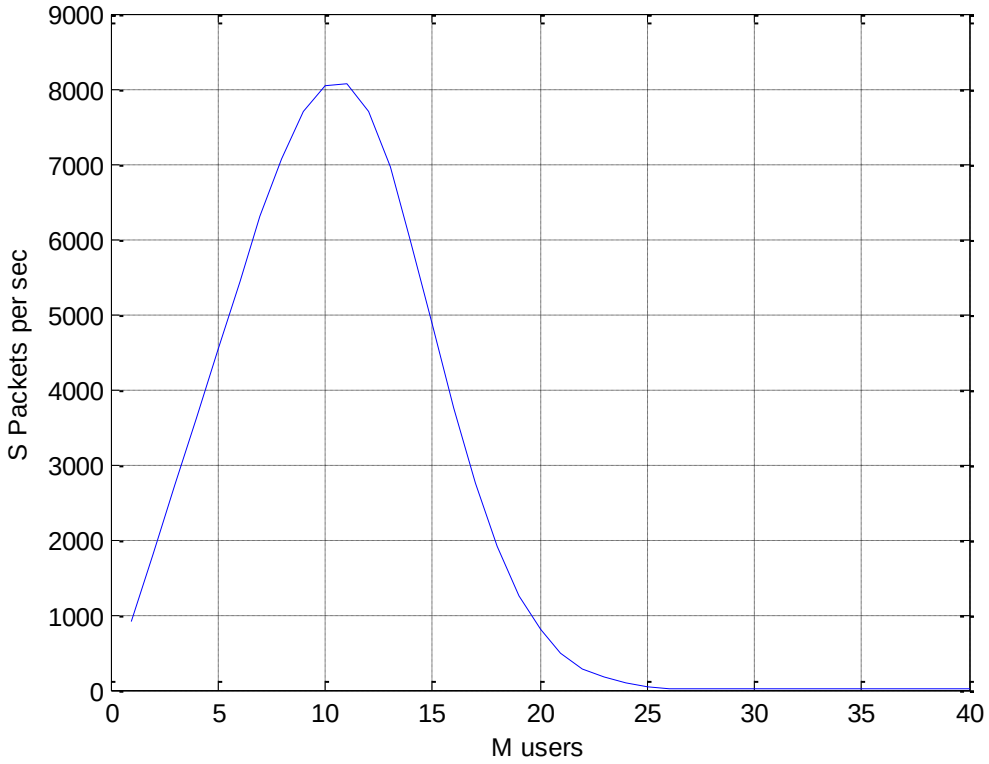

Figure 4.11 Throughput in packets per sec as a function of the number of users for the forward link, $R_b = 384$ kbps (bit rate) for data, for R = 175 km and h = 12 km, the activity factor is v = 1, packet length L = 424 bits and $n_{DL} = 0.9$.

4.4 Scenario 3

Figure 4.12 Map of Scenario 3, R = 100 km, h = 12 km.

In scenario 3 we reduce the radius of the cell to R = 100 km, as a result we expect an increase in the interference so a reduction of the capacity per cell, which is confirmed below. However, because the maximum number of the cells is greater, 19 in total, than in the other scenarios, it must be made clear if the total capacity of all the cells is greater than that of scenario 2. Moreover, because radius R is 100 km, scenario 3 is more realistic and can be utilized easily, because there will be a lower path loss and smaller latencies. As it was also mentioned in chapter 1, we suggest the use of repeater so that the already weakened signal could penetrate the aircraft, which due to its metal structure, will have a great penetration loss. However, the repeater will introduce some further delay, which increases synchronization issues which is expected to exist due to the fact that the radius of the cell is greater than the 35 km of normal cells. In Figure 4.12 we can see the map of Greece with the nineteen airports of for the third scenario with the directions of the sectors of the base stations. In Table 4.5, summarizes scenario 3.

	Base Stations	Antenna Directions in degrees	R
1	Athens (ATH)	50, 170, 290	100Km
2	Thessaloniki (SKG)	50, 170, 290	100Km
3	Heraklion (HER)	0, 120, 240	100Km
4	Rhodes (RHO)	60, 180, 300	100Km
5	Corfu (CFU)	0, 120, 240	100Km
6	Chania (CHQ)	80, 200, 320	100Km
7	Mytilene (MJT)	50, 170, 290	100Km
8	Argostolion (EFL)	0, 120, 240	100Km
9	Skiathos (JSI)	0, 120, 240	100Km
10	Alexandroupoli (AXD)	0, 120, 240	100Km
11	Kavala (KVA)	0, 120, 240	100Km
12	Karpathos (AOK)	0, 120, 240	100Km
13	Kalamata (KLX)	0, 120, 240	100Km
14	Limnos (LXS)	60, 180,300	100Km
15	Ikaria (JIK)	0, 120, 240	100Km
16	Milos (MLO)	0, 120, 240	100Km
17	Larissa (LRA)	0, 120, 240	100Km
18	Kastoria (KSO)	60, 180, 300	100Km
19	Agrinio	0, 120, 240	100Km

Table 4.7 Scenario 3: 19 Base Stations (BS) with one cell per BS and 57 sectors.

The analysis for scenario 3 is presented below which involves the capacity of the cells, namely the number of users M as a function of the bit number R_b for voice and packet data. Figure 4.13 presents results for scenario 3 with R = 100 km and h = 12 km. In order to calculate the capacity in the forward link, E_b/N_o values in Table 4.8 are used as before.

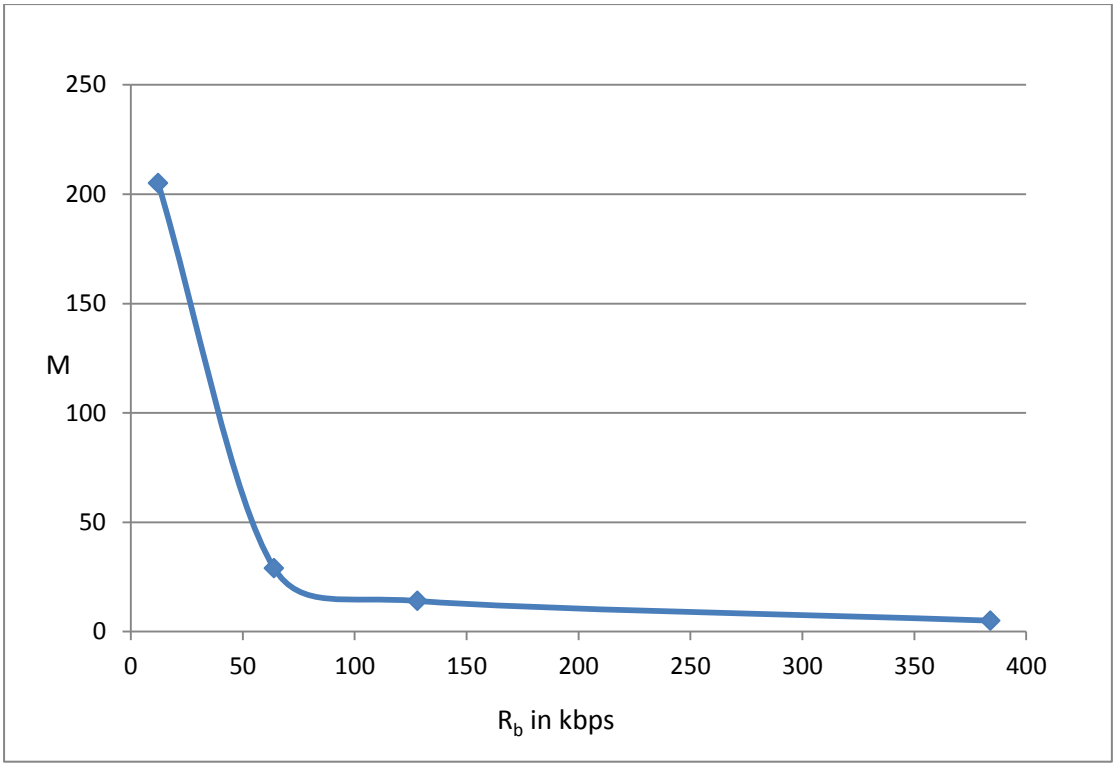

Figure 4.13 Number of users M for the forward link, as a function of the bit rate R_b (for voice R_b=12.2kbps and packet data R_b=64kbps, R_b=128kbps and R_b=384kbps) for R = 100 km and h = 12 km.

Table 4.8: Number of users M for the forward link, as a function of the bit rate R_b for voice and packet data, for R = 100 km, h = 12 km and n_{DL}=0.9. In the case of the voice service the activity factor is v=3/8+0.17

DPCCH overhead =0.375+0.17=0.545, while in the case of the data it is v=1.

Eb/No	6.92	5.01	5.01	4.90
Eb/No in dB	8.4	7	7	6.9
Rb (in kbps)	12.2	64	128	384
M	205	29	14	5

For the calculation of the capacity in the reverse link, E_b/N_o values in Table 4.9 are used as before. By comparing Tables 4.8 and 4.9, we can see that the limitation of the capacity of the system for voice or video call service which requires the symmetric

traffic in both links as in the former scenarios, is for the reverse link because of lower capacity.

So the final capacity of the Air – to – Ground system coincides with the capacity of the reverse link, Figure 4.14 and Table 4.9. In Table 4.10 the number of users per cells and the total number of users is presented for scenario 3 for voice call 12.2 kbps and video call services of 64 kbps and 128 kbps, which all concern symmetric traffic. Therefore the capacity of the cell is determined by the lowest value of the users for DL and UL. However, in the case of the data service there is no symmetric traffic because usually the forward link has significantly greater traffic than the reverse link. For data services we assume there will be the same three cases of users as those mentioned in scenarios 1 and 2.

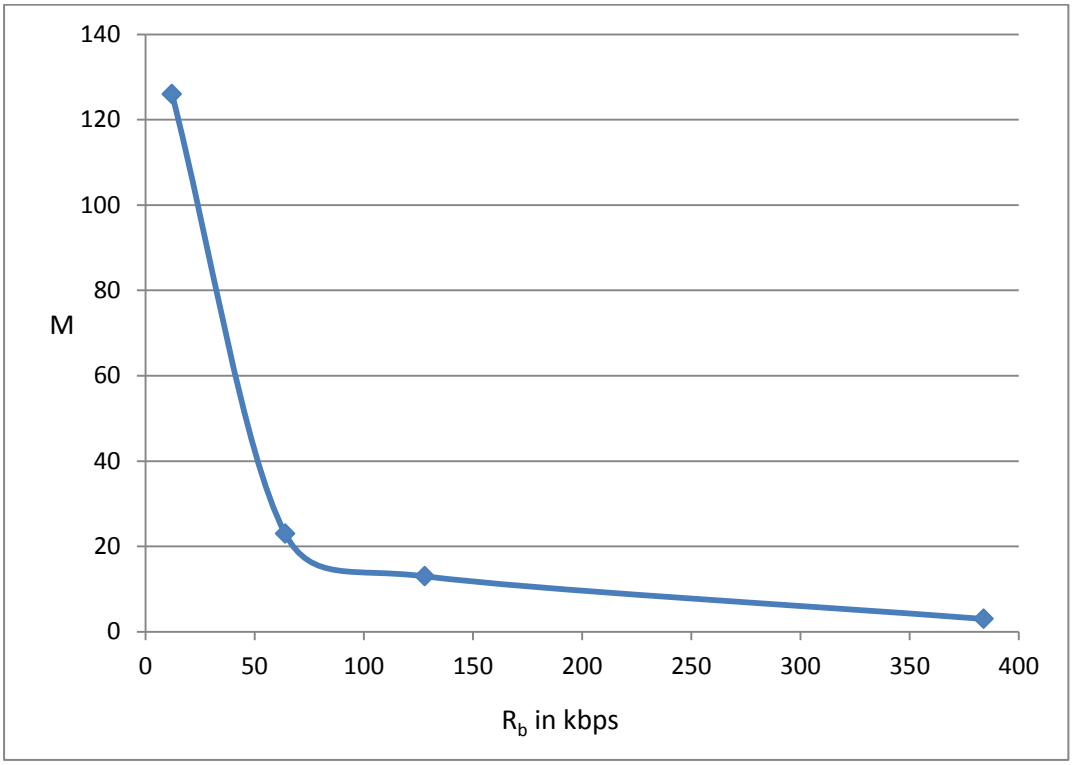

Figure 4.14: The number of users M for reverse link, as a function of the bit rate R_b (for voice R_b=12.2kbps and packet data R_b=64kbps, R_b=128kbps and R_b=384kbps) for R = 100 km and h = 12 km.

In Table 4.11 the number of users per cell and the total capacity for scenario 3 is depicted, for data service which all concern asymmetric traffic. n_{UL} and n_{DL} are assumed 0.9. By observing Table 4.11, for data service 12.2 kbps in the UL, we have 68 users, while in Table 4.10, for voice service 12.2 kbps in the UL, we have 126 users. This difference is due to the fact that in Table 4.11 for data service the activity factor is 1, while in Table 4.10 the voice service has activity factor 0.545.

E_b/N_o	5.62	3.16	2.81	3.16
E_b/N_o (in dB)	7.5	5	4,5	5
R_b (in kbps)	12.2 (voice)	64	128	384
M users per cell	126	23	13	3

Table 4.9 The number of users M for reverse link, as a function of the bit rate R_b for packet data for R = 100 km, h = 12 km and $n_{UL} = 0.9$.

Services	Voice call	Video call	
R_b (in kbps) for both DL and UL	12.2	64	128
M users per cell for DL	205	29	14
M users per cell for UL	126	23	13
M users per cell (min value from DL and UL)	126	23	13
Total users scenario 3	2394	437	247

Table 4.10 The number of users M for voice call and video call services – symmetric traffic, as a function of the bit rate R_b for DL and UL, for R = 100 km, h = 12 km, $n_{UL} = 0.9$ and $n_{DL} = 0.9$.

Services	data	data	data
R_b (in kbps)	64DL, 12.2UL	128DL, 64UL	384DL, 128UL
M users per cell for DL	29	14	5
M users per cell for UL	68	23	13
M users per cell (min value from DL and UL)	29	14	5
Total users scenario 3	551	266	95

Table 4.11 The number of users M for data services– asymmetric traffic, as a function of the bit rate R_b for DL and UL, for R = 100 km, h = 12 km, $n_{UL} = 0.9$ and $n_{DL} = 0.9$.

For symmetric traffic, by comparing Tables 4.5 and 4.10, we can notice that in scenario 3 the capacity per cell is lower than in the scenarios 1 and 2. This happens due to the fact that R is smaller and therefore greater interference. However, the total capacity that the 19 cells provide in scenario 3, is greater than the respective total capacity of the rest of the scenarios. For asymmetric traffic, by comparing Tables 4.6 and 4.11, in the same way we can notice that in scenario 3, the capacity per cell is smaller than in scenarios 1 and 2 but the total capacity of the scenario 3 is greater than in the other scenarios.

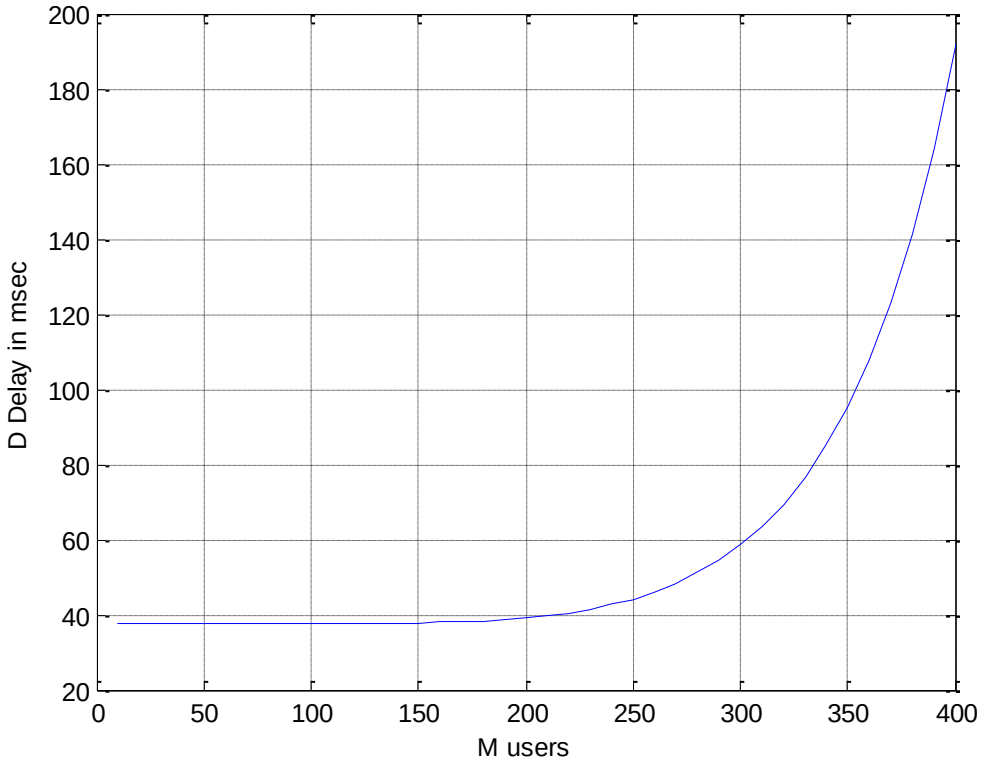

Figure 4.15 Delay D as a function of the number of users in the forward link, $R_b = 12.2$ kbps (bit rate) for voice, for R = 100 km and h = 12 km, the activity factor is v = 0.545, packet length L = 424bits, $t_d = 3$ msec.

Figure 4.15 shows delay D for the voice service $R_b = 12.2$ kbps. Therefore for scenario 3 the delay is D = 37.7772 msec, for M = 126 users per cell (see Table 4.9).

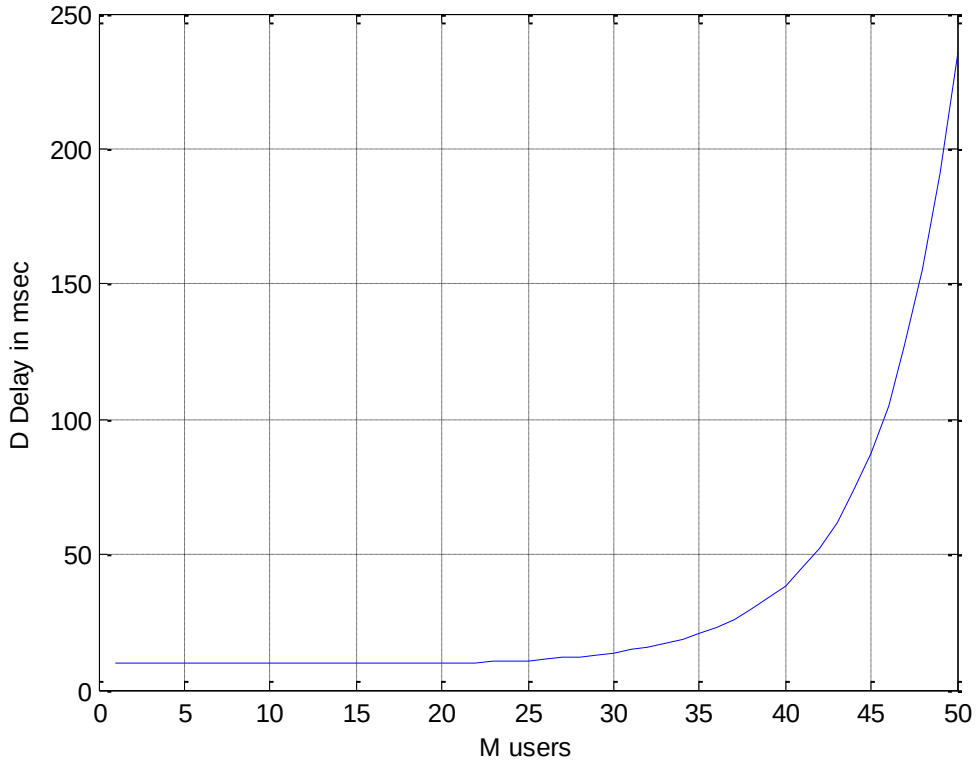

Figure 4.16: Delay D as a function of the number of users in the forward link, $R_b = 64$ kbps (bit rate) for data, for R = 100 km and h = 12 km, the activity factor is v = 1, packet length L = 424bits, $t_d = 3$ msec.

Figure 4.16 shows delay D for data service $R_b = 64$ kbps. Therefore for scenario 3 the delay for the symmetric traffic will be D = 10.3377 msec, for M = 23 users per cell (see Table 4.9), while in the asymmetric traffic (see Table 4.11), data service 64 DL & 12.2 UL the delay will increase to 12.9775 msec, if the users become 29.

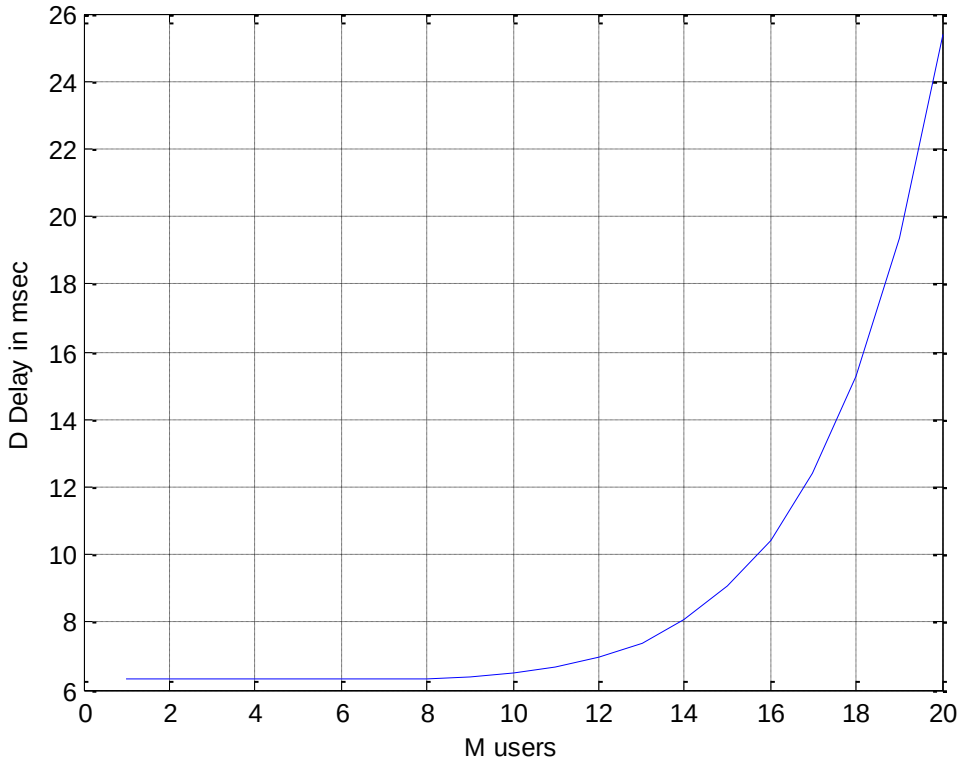

Figure 4.17: Delay D as a function of the number of users in the forward link, $R_b = 128$ kbps (bit rate) for data, for R = 100 km and h = 12 km, the activity factor is v = 1, packet length L = 424bits, $t_d = 3$ msec.

Figure 4.17 shows delay D for data service $R_b = 128$ kbps. Therefore for the scenario 3 the delay for the symmetric traffic, would be D = 7.3950 msec, for M = 13 users per cell (see Table 4.9), while for asymmetric traffic (see Table 4.11), data service 128 DL & 64 UL the delay will increase to 8.0678 msec, if the users become 14.

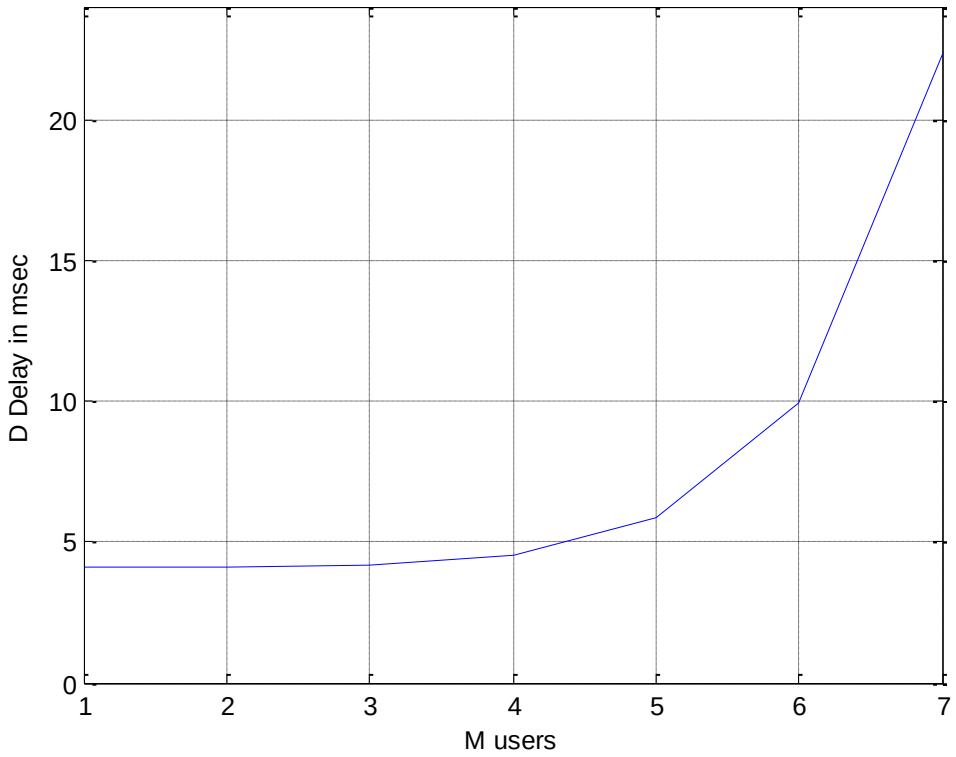

Figure 4.18 Delay D as a function of the number of users in the forward link, $R_b = 384$ kbps (bit rate) for data, for R = 100 km and h = 12 km, the activity factor is v = 1, packet length L = 424bits, $t_d = 3$ msec.

Figure 4.18 shows delay D for data service $R_b = 384$ kbps. Therefore for scenario 3 the delay for the symmetric traffic, will be D = 4.1485 msec, for M = 3 users per cell (see Table 4.9), while for asymmetric traffic (see Table 4.11), data service 384 DL & 128 UL the delay will increase to 5.8792 msec, if the users become 5.

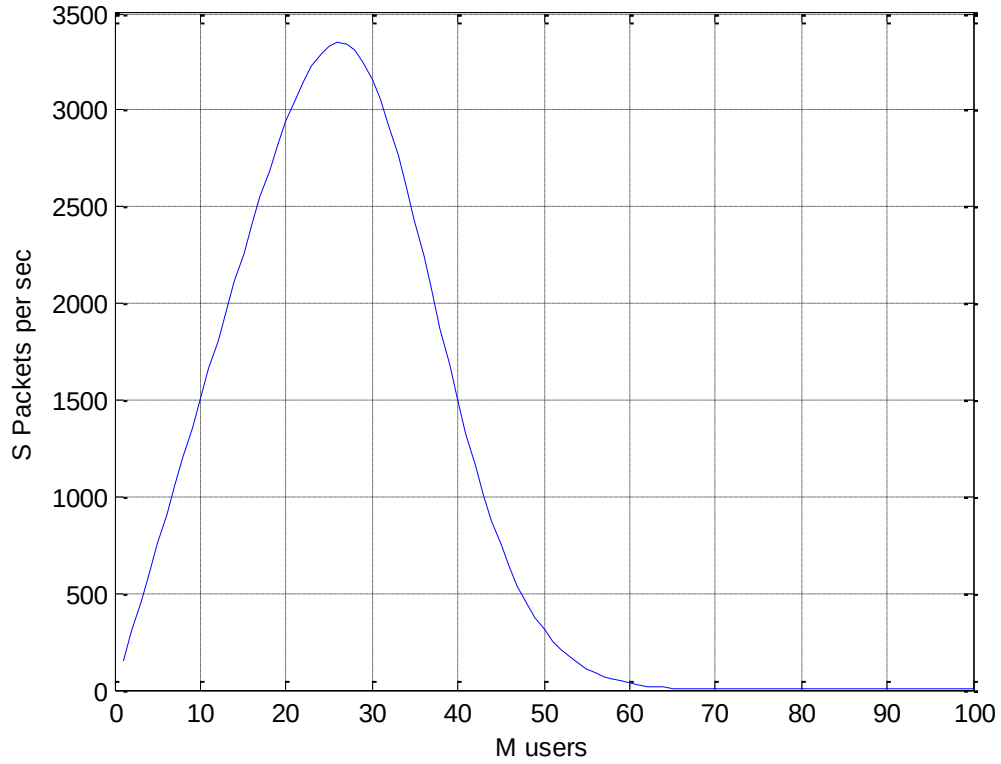

Figure 4.19: Throughput in packets per sec as a function of the number of users in the forward link, $R_b = 64$ kbps (bit rate) for data, for R = 100 km and h = 12 km, the activity factor is v = 1, packet length L = 424 bits and $n_{DL} = 0.9$.

As can be seen in 4.19, the throughput for the symmetric traffic of the video call (see Table 4.10), in the 64 kbps it would take its maximum value for M = 26 users and it would be 3350 packets per sec, however due to the reverse link the capacity is limited in the 23 users and the throughput is 3232 packets per sec. In the case of the asymmetric traffic (see Table 4.11), the maximum value of the throughput is utilized, 3350 packets per sec, for 26 users, because the maximum number of users in the data service 64 DL & 12.2 UL, is 29.

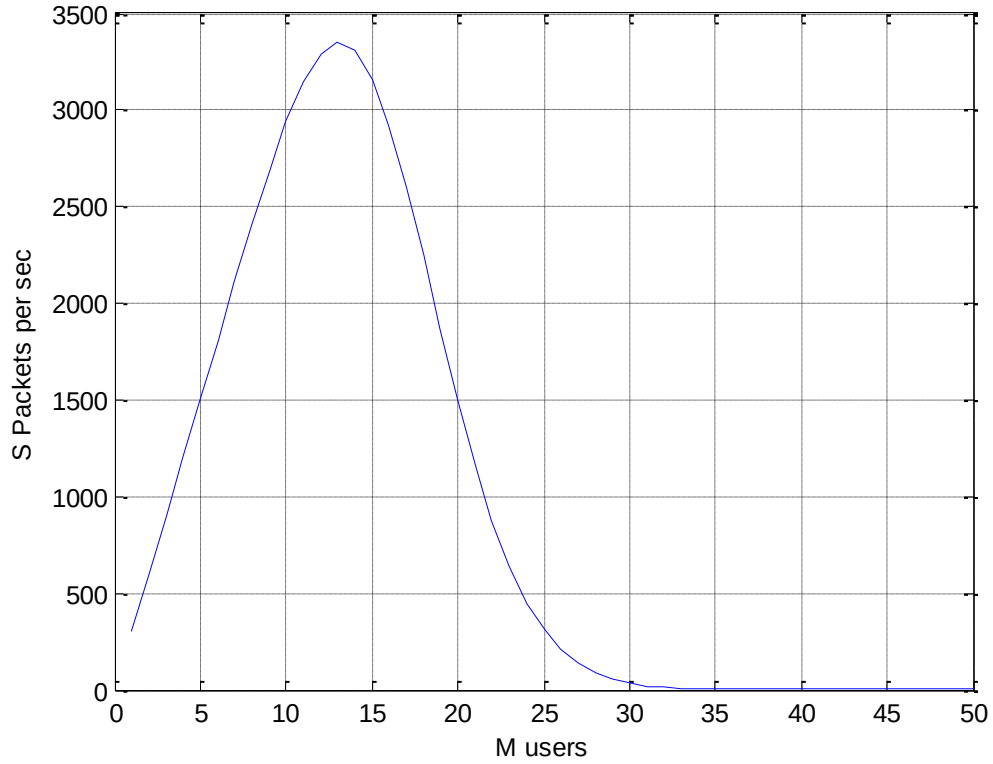

Figure 4.20 Throughput in packets per sec as a function of the number of users in the forward link, $R_b = 128$ kbps (bit rate) for data, for R = 100 km and h=12 km, the activity factor is v = 1, packet length L = 424 bits and $n_{DL} = 0.9$.

As it can be seen in Figure 4.20, the throughput for the symmetric traffic of the video call (see Table 4.10), in the 128 kbps it takes the maximum value for M = 13 users and it is 3350 packets per sec. In the reverse link the capacity is 13 users, as many as the number of users which is depicted in the maximum value of the throughput. In the case of the asymmetric traffic (see Table 4.11), we have the same throughput, 3350 packets per sec, for 13 users and the maximum number of users in the data service 128 DL & 64 UL, is 14.

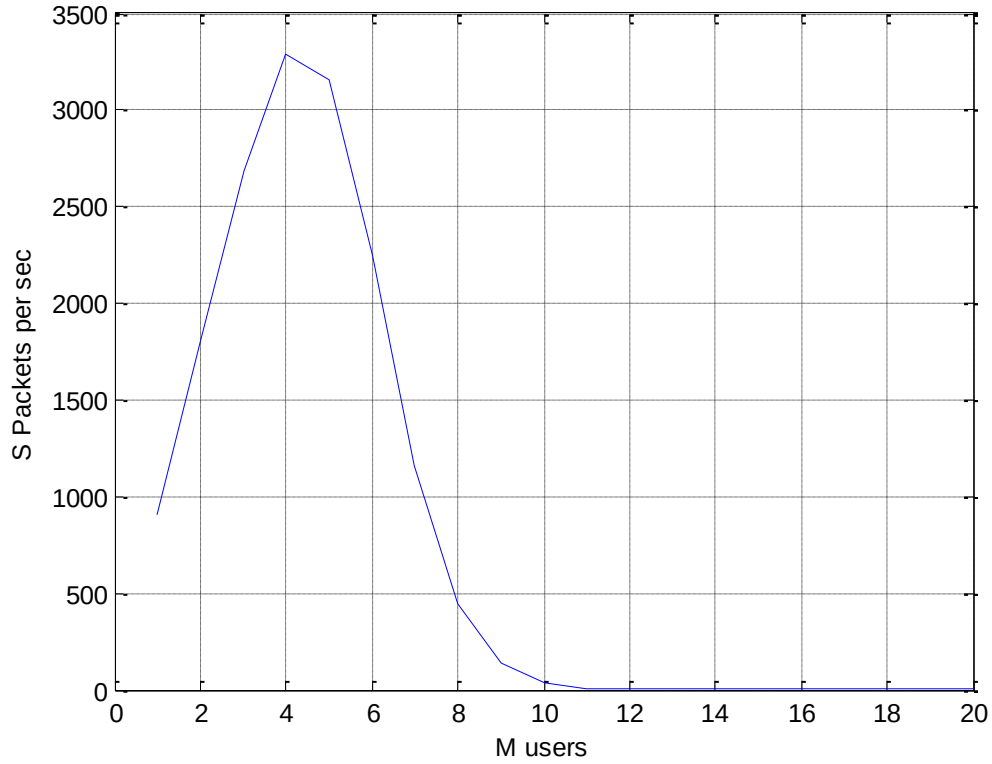

Figure 4.21 Throughput in packets per sec as a function of the number of users in the forward link, $R_b = 384$ kbps (bit rate) for data, for R = 100 km and h = 12 km, the activity factor is v = 1, packet length L = 424 bits and $n_{DL} = 0.9$.

As can be seen in 4.21 the throughput in the 384 kbps where there is only asymmetric traffic (see Table 4.11), the maximum value of the throughput is utilized, 3293 packets per sec, for 4 users, because the maximum number of users in the data service 384 DL & 128 UL, is 5.

4.5 General Remarks

It is obvious that the omnidirectional antennas would be uptilt (upwards tilt) and therefore there is coverage in high altitudes of flying. Near the Base Stations we will have coverage for both high and low altitudes of flying but as we wander off from the Base Station we won't have good coverage in low altitudes of flying due to the curvature of the earth and the natural obstacles of the morphology of the ground (mountains). If the airport is not close to its Base Station, it might not possible to serve subscribers in phase of landing and takeoff of aircrafts due to morphology of the

earth's surface and low altitude of the aircraft during that phase. In Chania airport in scenario 3 for example, the Base Station will be chosen in the western part of Crete, Kissamos, in order to reduce the overlapping with the Base Station of Heraklion airport. It is possible that this can be generally valid, namely the banning of calls during taking off and landing of the airplane, for the security of flights.

Base Stations in borders between countries will be designed in cooperation with respective countries so that the best solution can be found. Hence, for Mytilene and Rhodes, could be done in consultation with the airports of neighboring countries, which was assumed in our scenarios. The same is valid for the airports of Corfu, Thessalonica, Kastoria, Kavala and Alexandroupolis.

Among the cells it is fair that there will be overlapping so that there would be handover. When there is a greater overlapping than it is desired, this can be dealt with a lower power in the cell which creates the overlapping or less up-tilt. This can be better checked with the use of planning tools for Air-to-Ground communications and in future, when the cells are utilized in real calculations.

It is obvious that there will be difference between the nominal cell plan and the real utilization as exists in conventional terrestrial cellular systems.

We suggest the use of broadband repeater so that the already weakened signal can still penetrate the aircraft, which due to its metal structure will have a great penetration loss. The repeater, however, imports by itself some further delay, which increases the synchronization problem which is expected to exist due to the fact that the radius of the cell is greater than the 35 km of the normal cells. So the synchronization problem must be dealt with, maybe in a similar way as the extended cells were materialized for the coverage in the sea in terrestrial systems. The problem of power could be dealt by increasing the power of the base stations for the forward link and increased the power in the repeater for the reverse link. When an aircraft is approaching or departing from one base station, there will be power control both to the power of the base station, which serves him and the repeater of the aircraft. The pick antenna will be outside the aircraft e.g.at the back side and under the aircraft, while the service antenna will be in the aircraft and in front of so that there would be a greater isolation and the undesired oscillations of the signal will be avoided.

4.6 Summary

A case study has been made involving the study of the capacity of the Air – to - Ground system for the airports of Greece, in the three basic scenarios in which the number of the users, the delay and the throughput per cell is being calculated. In the first scenario, we restricted to the three major airports of the country, while in the second it expanded to six airports to provide radio-coverage for almost all Greece. In the first two scenarios the same cell radius of 175 km has been used, while in the third the radius was reduced to 100 km and the airports were increased to nineteen. In all three scenarios we assumed that all the users use the same service. The voice services were also studied for 12.2 kbps and data with transmission rates of 64, 128 and 384 kbps.

Chapter 5 Conclusions and future work

5.1 Conclusions

From the results for the OCIF in the forward and the reverse link we confirmed ourselves the results of Matolak [2] and Zhou [3], that the OCIF increases logarithmically with the maximum height of the cell and reduces as long as the radius of the cell becomes longer. The capacity of the cell is inversely proportional of the OCIF and therefore as long as the maximum height of the cell increases the users become fewer. Moreover, for the same reason the capacity increases as long as the radius of the cell increases. The results above are logical because as long as the radius of the cell increases and its maximum height is relatively low, then due to curvature of the earth we do not have line of sight from the interfering cells and so the interference is low, therefore the capacity increases.

From scenarios 1 and 2 which have the same cell radius 175 km, for the airports of Greece, it was found that we can service at the same time up to 179 voice subscribers per cell at bit rate 12.2 kbps which reduces to 33 users for video call of 64 kbps and in 18 for video call of 128 kbps. Moreover, for transmission data with bit rate 64kbps DL &12.2 kbps UL can be simultaneously serviced 71 subscribers per cell. The subscribers are reduced to 33 if the bit rate becomes 128 kbps DL & 64 kbps UL. And finally, they are reduced to 12 if the bit rate becomes 384 kbps DL & 128 kbps UL. Therefore scenario 2 which has the double number of cells, provides double total (for all Greece) capacity in relation to scenario 1.

In relation to delay, it has been noticed that the form of the chart with the users is stable up to a certain number of users and then it increases abruptly. Specifically for scenarios 1and 2 and bit rate 12.2 kbps the delay is almost 38ms and increases abruptly when the users become more than 500. For the bit rate 64 kbps the delay is almost 10 ms and increases abruptly when the users become more than 50. Moreover for bit rate 128 kbps the delay is almost 6.3msec and increases abruptly when the users become more than 25. Finally, for bit rate 384kbps the delay is about 4.1 ms and increases abruptly when the users become more than 10. The maximum value of throughput is a bit greater than 8000 packets per sec, for packet length 424 bits and becomes for 63 users when all the users have bit rate of 64 kbps. Similar maximum

value of the throughput is achieved for 32 users when they all have bit rate 128 kbps and 11 users when the bit rate becomes 384 kbps.

In scenario 3 which has cell radius 100km, it was found that we can serve at the same time until 126 voice subscribers per cell at bit rate 12.2 kbps which reduces to 23 users for video call of the 64 kbps and in 13 for video call of 128 kbps. Moreover, for data transmission at bit rate of 64 kbps DL & 12.2 kbps UL, 29 subscribers per cell can be served at the same time. The subscribers are reduced in 14 if the bit rate becomes 128 kbps DL & 64 kbps UL and finally, the users are reduced to 5 if the bit rate becomes 384 kbps DL & 128 kbps UL. In scenario 3 although the capacity per cell is lower than in scenarios 1 and 2, it provides greater total capacity (for all Greece) in relation to these scenarios.

With regard to the delay we noticed that the scenario 3 and for the bit rate 12.2 kbps the delay is almost 38 ms and it increases abruptly when the users become more than 200. For bit rate 64 kbps the delay is almost 10.3msec and increases abruptly when the users become more than 25. Moreover, for bit rate 128 kbps the delay is almost 7.4msec and increases abruptly when the users become more than10. Finally, for bit rate 384kbps the delay is almost 4.1msec and increases abruptly when the users become more than 4.

The maximum value of throughput is almost at 3300 packets per sec, for packet length 424 bits, and becomes for 26 users, when all users have bit rate 64kbps. The same almost maximum value of throughput is achieved for 13 users when all of them have bit rate 128 kbps and for 4 users when the bit rate becomes 384 kbps.

5.2 Future Work

As future work, one suggestion would be to study the capacity of the system, for more realistic scenarios in which it will not be obligatory all the users to have the same bit rate but we will have a number of users who will be using the simple voice service 12.2 kbps while others will be making video calls, while at the same time other users will be transferring data at different rates up to 384 kbps.

References

1. Viterbi, Principles of Spread Spectrum Communication, Addison-Wesley, 1995.

2. David W. Matolak, 3-D Outside Cell Interference Factor for an Air–Ground CDMA Cellular System, IEEE Transactions on Vehicular Technology, vol. 49, no. 3, pp. 706-710, May 2000.

3. J. Zhou, K. Ishizawa, and H. Kikuchi, Forward link performance of data packet transmission in an aeronautical CDMA cellular system, IEICE Trans. Commun., vol.E88-B, no.2, Feb. 2005, pp. 826-830.

4. B. Smida, V. Tarokh, Analysis of Interference in Air-to Ground CDMA Cellular Systems Under Idealized Assumptions, IEEE Transactions on Communications, vol. 59, no. 1, pp 258-267, Jan 2011.

5. J. Zhou; W. Pan; Y. Onozato, On the Capacity and Outage Probability of an Air-Ground CDMA Cellular System with Imperfect Power Control, Proceedings of International Conference on Wireless Communications, Networking and Mobile Computing, 2007, pp. 662 – 665.

6. S. Elnoubi, Three-Dimensional Cellular Systems for Air/Ground Personal Communication, IEEE Transactions on Vehicular Technology, vol. 54, no. 6, pp. 1923-1931, Nov 2005.

7. M. C. Ramon, R. M. Rodrigez-Osorio, B. T. Ahmed, J. J. Iglesias Jimenez, Capacity of a UMTS System for Aeronautical Communications, Proceedings of 11th WSEAS Int. Conference on Communications, Agios Nikolaos, Crete, Greece, July 26-28, 2007.

8. Harri Holma and Antti Toskala, WCDMA for UMTS – HSPA evolution and LTE, 4th Edition, John Wiley & Sons, 2007.

9. S.A. Mawjoud, A. T. Hussien, Capacity Enhancement In WCDMA Cellular Network, Al-Rafidain Engineering journal, Vol. 20, No. 1, Feb 2012.

10. Law_of_cosines, http://en.wikipedia.org/wiki/Law_of_cosines

11. B. T. Ahmed, M. C. Ramon and L. H. Ariet, The capacity of Air –Ground W-CDMA system (UpLink Analysis), 13th IEEE International Symposium on Personal, Indoor and Mobile Radio Communications, 2002.

12. Phase-Shift Keying - wiki, http://en.wikipedia.org/wiki/Phase-shift_keying

13. P. Singla, J. Saxena, Enhanced Capacity Analysis in WCDMA System, International Journal of Electronics and Communication Engineering, International Research Publication House, Vol. 4, Number 1, pp. 69-82, 2011.

14. http://www.iitg.ernet.in/engfac/krs/public_html/lectures/ee635/A3.pdf

15. http://www.prokerala.com/travel/airports/distance/ Airport Distance Calculator

16. http://www.boeing.com/boeing/commercial/cabinair/environmentfacts.page

    Commercial Airplanes

17. http://traveltips.usatoday.com/altitude-plane-flight-100359.html What Is the Altitude of a Plane in Flight?

18. http://www.fearofflyingphobia.com/flysohigh.html Why Do Planes Fly So High?

19. http://www.comlab.hut.fi/studies/3275/Cellular_network_planning_and_optimization_part8.pdf Cellular Network Planning and Optimization Part VIII: WCDMA link budget, Jyri Hämäläinen, 2008.

20. Controller–pilot data link communications, http://en.wikipedia.org/wiki/Controller%E2%80%93pilot_data_link_communications

21. M. E. Johnson and G. D. Gierhart, "An atlas of basic transmission loss (0.125, 0.3, 1.2, 5.1, 9.4, 15.5 GHz)", National Technical Information Service, DOT Rep. FAA-RD-80-1, Springfield, VA, 1980.

22. Horizontal Antenna Pattern of 65 Degree Beamwidth, http://www.air802.com/sector-antenna-dual-band-2.4-and-5.1-to-5.8-ghz-dual-band-two-n-connectors.html

23. M. C. Ramon, R. M. Rodrigez-Osorio, B. T. Ahmed, J. J. Iglesias Jimenez, Capacity of a UMTS System for Aeronautical Communications, Proceedings of 11th WSEAS Int. Conference on Communications, Agios Nikolaos, Crete, Greece, July 26-28, 2007.

24. Jialin Zou, V. K. Bhargava, Qiang Wang, Reverse Link Analysis and Performance Evaluation for DS-CDMA Cellular Systems, Department of Electrical and Computer Engineering University of Victoria, Victoria, B.C. Canada V8W 3P6.

Appendix A

Errors in Matolak's formula for r_i

The correct formula, as with Smida [4] and formulation in this dissertation, relationship (2.21) is

$$r_i = \sqrt{D_i^2 + r^2 + z^2 + 2r(x_i \cos\varphi + y_i \sin\varphi)} \quad \text{(A.1)}$$

While on Matolak's paper r_i is given by:

$$r_i = \sqrt{D_i^2 + r^2 - 2r(x_i \cos\varphi + y_i \sin\varphi)} \quad \text{(A.2)}$$

If we assume that it is valid and that formula (A.2) of Matolak the following relationship should be valid: from equation (A.1) and (A.2)

$$z^2 + 2r(x_i \cos\varphi + y_i \sin\varphi) = -2r(x_i \cos\varphi + y_i \sin\varphi)$$

$$z^2 = -4r(x_i \cos\varphi + y_i \sin\varphi) \quad \text{(A.3)}$$

If in relationship (A.3) we try to replace the (2.23) we will get:

$$z^2 = -4r(-D_i \cos\theta_i)$$

$$z^2 = 4rD_i \cos\theta_i \quad \text{(A.4)}$$

The $z \geq 0$ and the $z^2 \geq 0$, $r \geq 0$ $D_i > 0$ while the $\cos\theta_i$ will also be able to take negative value for angles of $90^o < \theta_i < 270^o$

e.g. for $r>0$, $D_i > 0$, $z^2 > 0$ and $\theta_i = 100^o$

formula (A.4) is not valid because $\cos(100^o) = -0.173$ namely negative. So the relationship (A.2) of Matolak is not valid. (probably a printing mistake)